Contract No:

This document was prepared in conjunction with work accomplished under Contract No. DE-AC09-08SR22470 with the U.S. Department of Energy (DOE) Office of Environmental Management (EM).

Disclaimer:

We put science to work.™

Savannah River National Laboratory™

OPERATED BY SAVANNAH RIVER NUCLEAR SOLUTIONS

A U.S. DEPARTMENT OF ENERGY NATIONAL LABORATORY • SAVANNAH RIVER SITE • AIKEN, SC

Crystallization in High-Level Waste Glass: A Review of Glass Theory and Noteworthy Literature

J. H. Christian

August 2015

SRNL-STI-2015-00415, Revision 0

SRNL.DOE.GOV

DISCLAIMER

Printed in the United States of America

Prepared for
U.S. Department of Energy

SRNL-STI-2015-00415
Revision 0

Keywords: *high level waste, vitrification, crystallization, spinel, nepheline, liquidus*

Retention: *Permanent*

Crystallization in High-Level Waste Glass: A Review of Glass Theory and Noteworthy Literature

J. H. Christian

August 2015

Prepared for the U.S. Department of Energy under contract number DE-AC09-08SR22470.

Savannah River National Laboratory™
OPERATED BY SAVANNAH RIVER NUCLEAR SOLUTIONS

REVIEWS AND APPROVALS

AUTHORS:

J. H. Christian, Process Technology Programs Date

TECHNICAL REVIEW:

C. M. Jantzen, Process Science and Engineering Section Date

K. M. Fox, Hanford Support Missions Date

APPROVAL:

E. N. Hoffman, Manager Date
Process Engineering Technology Group

A. P. Fellinger, Manager Date
Environmental & Chemical Process Technology Research Programs

C. C. Herman, Director, Hanford Support Missions Date

EXECUTIVE SUMMARY

There is a fundamental need to continue research aimed at understanding nepheline and spinel crystal formation in high-level waste (HLW) glass. Specifically, the formation of nepheline solids ($K/NaAlSiO_4$) during slow cooling of HLW glass can reduce the chemical durability of the glass, which can cause a decrease in the overall durability of the glass waste form. The accumulation of spinel solids ($(Fe, Ni, Mn, Zn)(Fe,Cr)_2O_4$), while not detrimental to glass durability, can cause an array of processing problems inside of HLW glass melters. In this review, the fundamental differences between glass and solid-crystals are explained using kinetic, thermodynamic, and viscosity arguments, and several highlights of glass-crystallization research, as it pertains to high-level waste vitrification, are described. In terms of mitigating spinel in the melter and both spinel and nepheline formation in the canister, the complexity of HLW glass and the intricate interplay between thermal, chemical, and kinetic factors further complicates this understanding. However, new experiments seeking to elucidate the contributing factors of crystal nucleation and growth in waste glass, and the compilation of data from older experiments, may go a long way towards helping to achieve higher waste loadings while developing more efficient processing strategies. Higher waste loadings and more efficient processing strategies will reduce the overall HLW Hanford Tank Waste Treatment and Immobilization Plant (WTP) vitrification facilities mission life.

TABLE OF CONTENTS

LIST OF TABLES

LIST OF FIGURES

LIST OF ABBREVIATIONS

Ac	Acmite
CCC	Centerline Canister Cooling
DWPF	Defense Waste Processing Facility
DOE	The United States Department of Energy
DSC	Differential Scanning Calorimetry
DTA	Differential Thermal Analysis
Ds	Disilicate
EDS	Energy Dispersive Spectroscopy
T_g	Glass Transition Temperature
GCM	Glass Composite Materials
HLW	High-Level Waste
KJMA	Kolmogorov-Mehl-Johnson-Avrami Equation
T_L	Liquidus Temperature
LAW	Low-Activity Waste
MRO	Medium-Range Order
NE	Nepheline
OSPE	Octahedral Site Preference Energy
PCCS	Product Composition Control System
PCT	Product Consistency Test
RDF	Radial Distribution Function
SRNL	Savannah River National Laboratory
SRS	Savannah River Site
SEM	Scanning Electron Microscopy
SRO	Short-Range Order
NAS	Soda-Alumina-Silica
T_m	Melting Temperature
TTT	Time-Temperature Transformation
WTP	Hanford Tank Waste Treatment and Immobilization Plant
XRD	X-ray Diffraction

1.0 Introduction

Ostensibly, the distinction between glasses and solid crystals is a hard one to make. The outward appearance of glass is essentially solid-like and many of the glass properties (e.g. thermal, mechanical, density) are similar to those of solid crystals[1]; however, there exist several fundamental differences between the two. Understanding these differences is vital for glass technology at all levels of complexity, whether it's in designing glass-ceramic cookware for our kitchens[2], making optical fibers to carry information with large bandwidths[3], recycling industrial waste[2a], or immobilizing high-level nuclear waste (HLW) through vitrification at places like the Defense Waste Processing Facility (DWPF) in Aiken, SC and the Hanford Tank Waste Treatment and Immobilization Plant (WTP) in Richland, WA.[4]

Borosilicate waste glasses and melts, like natural silicate glasses and melts, possess short-range order (SRO; radius of influence ~ 1.6–3 Å) around a central atom, e.g. polyhedra such as tetrahedral and octahedral structural units.[5] Glasses also possess medium-range order (MRO)[5] which encompasses second- and third-neighbor environments around a central atom (radius of influence B3–6 Å). The more highly ordered regions in glass, referred to as clusters or quasicrystals, often have atomic arrangements that approach those of crystals[5,6], however, they do not possess long-range ordering (LRO) like crystalline solids.

Despite the many fundamental differences between glasses and crystals, the two are intimately linked atomistically since nearly all glass forming materials can be crystallized, and virtually all crystalline materials can be melted into glass. The latter transformation can occur if a poor glass forming material is cooled so rapidly from a melt that insufficient time is provided to allow the reorganization of the structure into the periodic arrangement required by crystallization. The conditions for this transformation are extreme and thus the formation of a glass from a predominately crystal-forming material is typically only observed under highly controlled conditions.[7] Conversely, the formation of crystals from glass-forming materials can occur readily under practical thermal and chemical conditions when the solubility of a species is exceeded in the glass.[8] In fact, the controlled crystallization of glass has been exploited for over fifty years, since it's accidental discovery in 1957[2b], and has resulted in countless consumer, optical, electrical, and architectural goods, such as thermal shock resistant cookware and cooktops[9], improved dental implants[10], and enhanced magnetic media hard disks components.[11] Indeed, the discovery of controlled crystallization in glass, sparked a revolution in both glass and ceramic science.

Although there are clearly many applications that seek to utilize the crystallization of glass in order to engineer materials with desired properties, there are also a large number of applications in which crystallization of glass is highly undesirable, the most prevalent example being in window glass, where clarity and transparency are indispensable properties. The glass used in microscope lenses is another example in which non-crystalline glass is desired. Additionally, there are many facets of HLW vitrification that can be hindered due to crystallization. Specifically, the formation of nepheline solids ($K/NaAlSiO_4$) can reduce the chemical durability of glass, which can result in decreased waste form durability. Furthermore, the accumulation of spinel solids ($(Fe, Ni, Mn, Zn)(Fe,Cr)_2O_4$), while not detrimental to glass durability[12], can cause an array of problems inside of HLW glass melters.

Increasing the mass fraction of waste components in the glass (i.e. increased waste loading) above their solubility limit can foster crystallization in HLW glass; however higher waste loading is desirable because it allows more waste to be processed in a smaller disposal volume, thereby reducing storage, disposal, and operating costs. Although it is difficult to develop robust, predictive models of HLW glass crystallization behavior due to the compositional complexity of HLW, it is possible, and it is therefore vital to continue lab-scale research on the subject, and to continue to evaluate and update the currently used models based on new data and/or changes to the process flowsheet.

Without fundamental scientific research on HLW vitrification, the process control models used to set operation protocols at DWPF and WTP are subjected to constraints that can limit waste loading below its capacitive level. These process and product constraints, which have 5% uncertainty applied, are designed to develop a durable, high-quality waste product while avoiding a major malfunction in the HLW vitrification operations. Currently at DWPF, the waste loading of spinel formers is at the maximum concentration that will not allow precipitation of spinel crystals in the melter. However, recent pilot-scale studies at PNNL have explored the effects of exceeding this waste solubility limit, thereby allowing crystallization to occur in a melter.[13] It has been suggested that this strategy may help to increase waste loading at WTP, although the extent of the negative impacts of operating a melter under a crystal-tolerant environment, have yet to be fully explored. Therefore, continuation and improvement of HLW research is necessary to develop new methods for achieving higher waste loadings while also minimizing unwanted glass behavior (e.g. nepheline crystallization during slow canister cooling and spinel crystallization in the HLW melter), and to develop strategies to minimize the undesired effects of working in glass compositional space where crystallization can occur. Research-derived improvements to the vitrification process, like the development of a robust liquidus model in 2006-07 by Jantzen et al.[14], and the nepheline discriminator by Li et al. in 2003[4c], have the potential to translate into significant cost savings by reducing mission life or disposal costs.

With this in mind, this review compiles several highlights of glass-crystallization research as it pertains to HLW vitrification. It starts by explaining the fundamental differences between glass and solid-crystals using kinetic, thermodynamic, and viscosity arguments. Next, some highlights of the many problems associated with crystallization as it pertains to HLW glass are provided, followed by highlights of research on spinel and nepheline crystallization in HLW glass. Lastly, the review concludes by posing several questions and experiments, which would be useful towards better understanding crystallization during HLW vitrification. The review is written to provide glass and ceramic researchers with an overview on the current state of crystallization in HLW glass in order to facilitate the development of future glass crystallization studies.

2.0 Explaining the Differences Between Glass and Solid-Crystals

To comprehend the principles of glass crystallization it is necessary to understand why glasses remain amorphous when they are cooled below the melting temperature(s) of their crystalline phase(s) instead of crystallizing. In this section, the different processes by which glass and solid-crystals form is explained using kinetic, thermodynamic, and viscosity arguments. Importantly, the fundamentals of glass formation and crystallization is often different in commercial glasses than in HLW glasses, since HLW glasses always contain melt insolubles and refractory surfaces that act as nucleation sites for what is called heterogeneous crystallization.

The formation of glass is most easily visualized using the volume-temperature diagram shown in Figure 2-1.[15] This diagram considers a small volume of a liquid material at point A. Upon cooling, the volume of the liquid steadily decreases until the liquid reaches its melting point (T_m). At this point the liquid can proceed towards one of two different states depending on its cooling rate. A liquid crossing its standard freezing point will crystalize in the presence of a seed crystal or nucleus around which a crystal structure can form thereby creating a solid. Lacking any such nuclei, the liquid phase can be maintained all the way down to the temperature at which crystal homogeneous nucleation occurs. Homogeneous nucleation can occur above the glass transition temperature, but if homogeneous nucleation has not occurred above that temperature, an amorphous (non-crystalline) solid will form. If the material readily forms a crystal then its volume will decrease sharply as the atoms in the material undergo long-range ordering into an efficiently packed crystal. In glass forming liquids, like a silica-melt, crystallization does not occur below T_m, because the liquid is not given enough time to nucleate, i.e. the liquid is supercooled. As the liquid proceeds into a supercooled state, the volume shrinks slowly by rearrangement of the liquid atoms. Ultimately, as the liquid is cooled further, the viscosity increases sharply. This increase in viscosity eventually becomes so great that the atoms can no longer completely rearrange to form a crystal structure. At this point the atoms become locked into the position they were in at the moment the viscosity became too great for them to move. This is known as the glass transition point or temperature (T_g). Thus, the rate of cooling and the volume/viscosity changes in a liquid are essential in determining whether a liquid cools into a glass or crystalline solid.

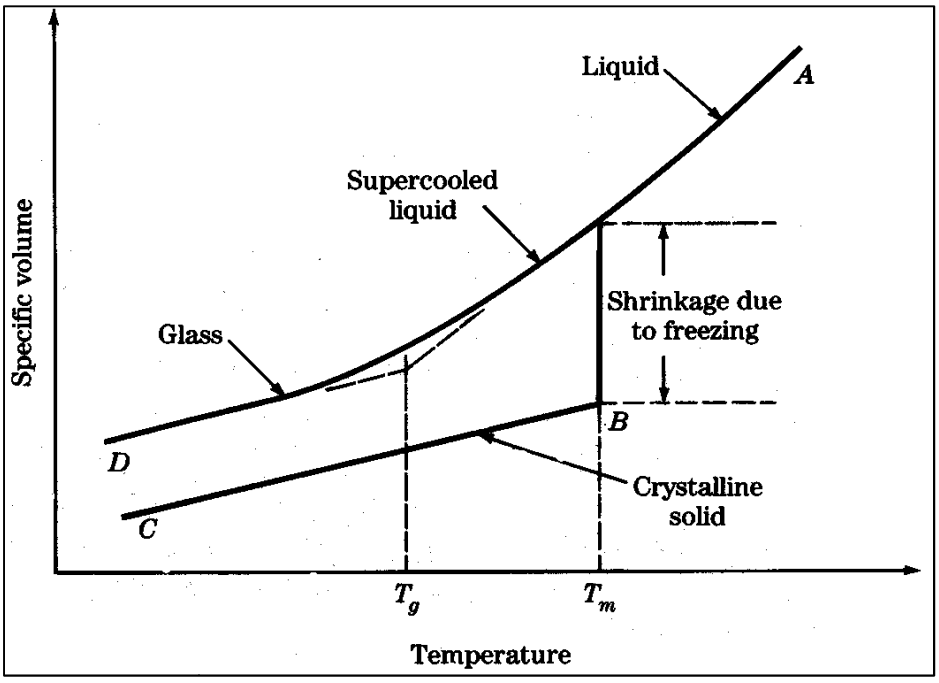

Figure 2-1. The volume-temperature diagram of a glass-forming and crystal-forming liquid.

Using a kinetic argument, one can devise a simple glass classification system, where any compound or mixture that can form a glass by cooling from the melt at a moderate rate is considered to be a good glassformer. Materials that require a fast cooling rate in order to form a glass are considered to be poor glassformers, and melts which cannot be cooled to form glasses without the use of extreme cooling rates are considered to be non-glassformers.[16]

Crystallization, in fact, refers to a two-step process, namely, nucleation and growth. Specifically, crystallization requires the presence of a nucleus on which the crystal will subsequently grow to a detectable size.[1] In the nucleation stage, small, stable volumes of the crystalline phase are formed. These phases can form either homogeneously, i.e. spontaneously within the melt, or heterogeneously, i.e. the nuclei form at pre-existing surfaces, which can exist due to insoluble impurities, the melting vessel interface, bubbles, etc.[16] If no nuclei are present in a system then crystallization cannot occur and the material will form a glass upon cooling below its glass transition temperature. If some nuclei are present then the crystal growth stage can commence. Growth involves the movement of atoms or molecules from the glass, across the glass-crystal interface, and into the crystal. The driving force for this process is the difference in volume between the glass and crystalline states.[1]

As stated above, all HLW glasses are processed in the presence of nucleation sites, such as melt insolubles like RuO_2, RhO_2, Ag, and Pt, and refractory surfaces in the melter and/or riser. Therefore, crystallization in HLW glass is always heterogeneous.[17],[18],[19] For this reason, only heterogeneous nucleation is described here. For a discussion of homogeneous nucleation see Appendix A.

Crystallization is dominated by the growth phase in heterogeneous systems, because the energy barrier for growth to commence, ΔG^*, is much lower in heterogeneous systems than in homogeneous systems. As shown in Figure 2-2, the addition of new molecules to nuclei larger than a critical radius of r* (i.e. crystal growth) results in a decrease in the free energy of a system. Therefore, once a stable nucleus exceeds the critical size of r*, the growth stage of crystallization will occur spontaneously.

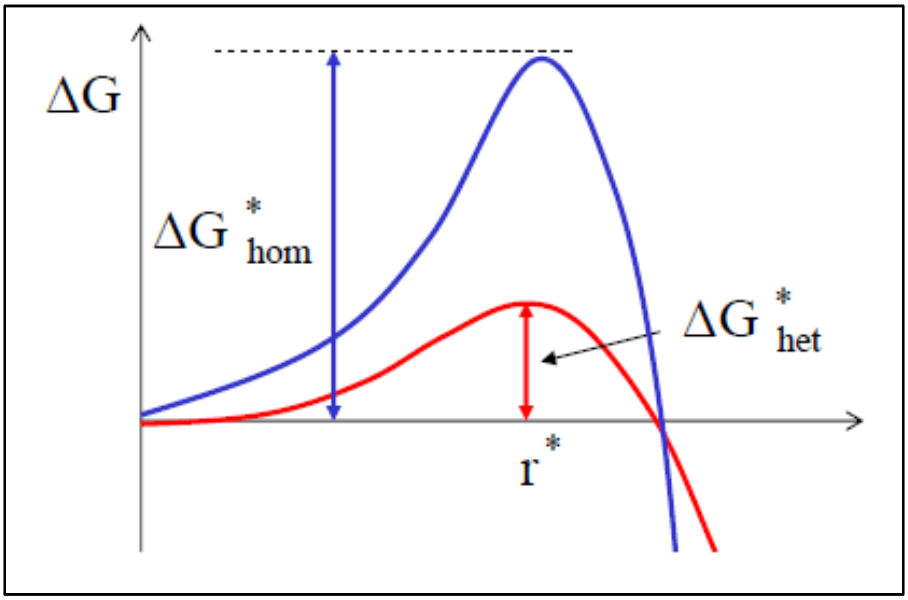

Figure 2-2. The Gibbs free energy (ΔG) is plotted as function of the radius (r) of a spherical nucleation site. r* represents the critical radius of a nucleus. Above this critical size, the Gibb's free-energy decreases as the nucleus grows, thus ΔG* is the energy barrier for formation of a solid nucleus of size r*. Above this barrier the growth stage of crystallization will commence.

Because the energy needed to generate a stable nucleus with a radius of r* is smaller in heterogeneous systems than in homogeneous ones, heterogeneous crystallization also starts at a lower undercooling than homogeneous crystallization, as depicted in Figure 2-3. Therefore, heterogeneous systems have a much smaller undercooling buffer zone between the melting temperature, T_m, and the point at which crystallization begins. The presence of this small buffer zone is one of the many difficulties faced in attempting to avoid crystallization in heterogeneous systems.

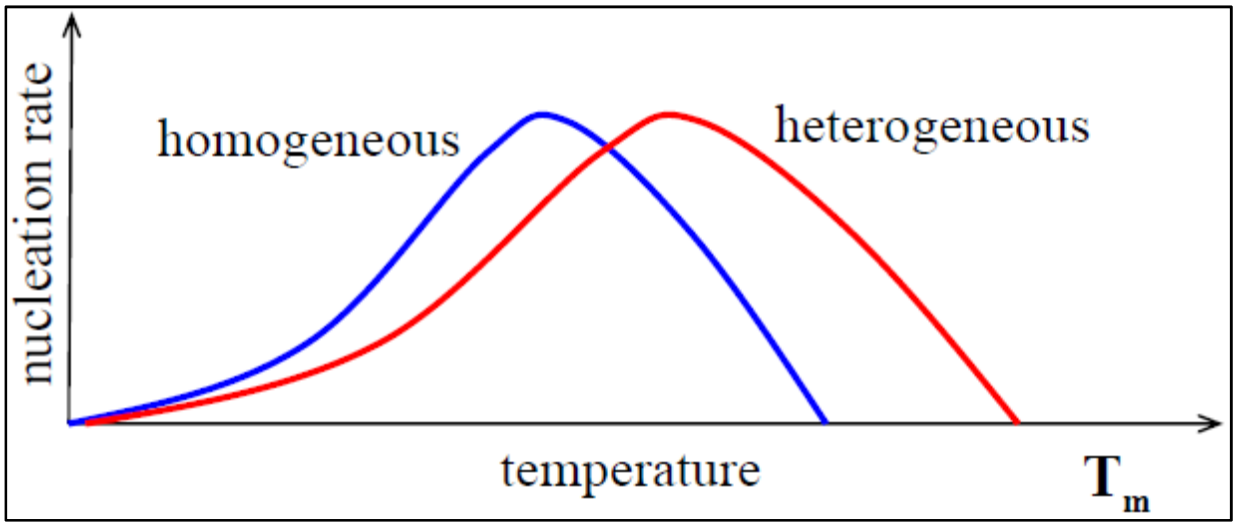

Figure 2-3. The nucleation rates in a heterogeneous and homogeneous system are shown as a function of temperature. T_m is the melting temperature. In heterogeneous systems a smaller undercooling zone exists than in homogeneous systems, thus crystallization can commence close to the melting temperature.

The next section highlights the many problems associated with the formation of solid crystals during HLW vitrification.

3.0 Potential Problems Associated with Crystallization in High-Level Waste Glass

At the Savannah River Site (SRS), waste from defense material production has been immobilized in glass since 1996. Currently, ~7500 tons of glass, filling over 3,928 canisters, has been produced, thus immobilizing over 55 megacuries of radioactivity. Nearly all commercial glasses contain multiple components such as fluxes to lower the glass processing temperature, and property modifiers to strengthen the glass network. However, nuclear waste glasses contain these species (both from frit and from the waste) and nearly every other element of the periodic table. Thus, they are outstanding examples of highly complex multicomponent glasses.[20] The composition of the HLW glass, often being high in Al_2O_3 and transition metal oxides, readily provides a chemical environment that is conducive to crystallization. Furthermore, the compositional region in sludge space at the Hanford site is much broader than at SRS, and control over crystallization while achieving high waste loading will be challenging.

During melting of batch materials, the ionic salts will melt quickly, forming low-temperature eutectics, while hydroxides and nitrates tend to react with boron oxide, silica, and other glass forming components, to release large amounts of gas.[21] Additionally, sulfates and halides will either dissolve in the glass-forming melt, partly evaporate or decompose, or partly segregate.[21]

Wastes high in both Na_2O and Al_2O_3 tend to precipitate nepheline ($NaAlSiO_4$) during slow cooling (as described in detailed in Section 5).[22] Waste with zirconia may first form solid zirconium silicate, sodium-zirconium silicate, or rare-earth zirconates before dissolving in the molten glass.[23] In melts with a reducing flowsheet and a large content of iron or manganese, the Fe^{3+} and Mn^{4+} oxides and hydroxides reduce to Fe^{2+} and Mn^{2+} and release O_2. This may occur at DWPF, but not at WTP where the oxygen partial pressure of the melt will be zero as the melt pool will be air sparged. A comparison of the stability among Fe and Mn oxides as a function of temperature and oxygen partial pressure is shown in Figure 3-1. Additionally, nuclear wastes typically contain redox sensitive noble metals such as Pd, Rh, and Ru.[21] Their oxides may precipitate in the form of needle-shaped crystals. Furthermore, RuO_2 does not dissolve in the melt, and provides nucleation sites for the formation of a variety of crystals.[24] Thus, preventing crystallization in HLW glass is a difficult challenge

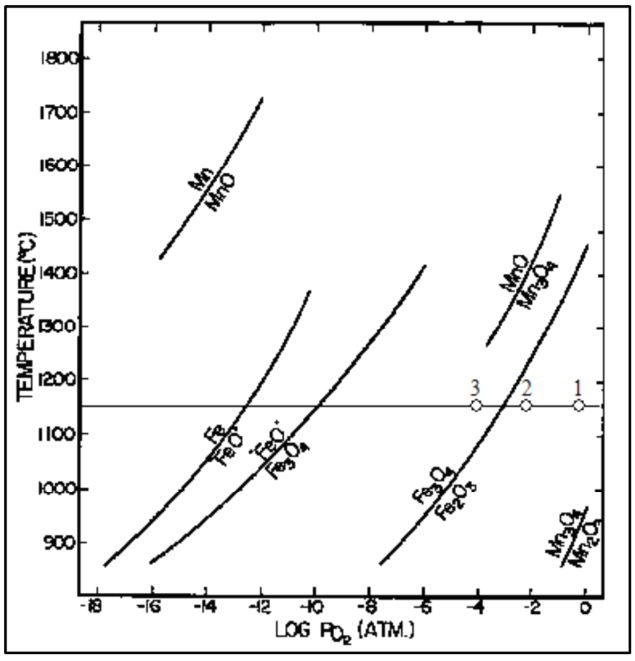

Figure 3-1. Comparison of stability among the oxides of iron and manganese as a function of temperature and oxygen partial pressure.[25]

Crystallization of HLW glass can be problematic during canister cooling due to the slow cooling rates experienced in the center of the canister. Additionally, crystal formation in a melter can cause a melt to be non-Newtonian, thus creating difficulty in the melter and in discharging from the melter to the canister. The non-Newtonian viscosity of the melt can cause viscosity to change in an unpredictable manner. Unpredictable changes to HLW melt viscosity, specifically unpredictable increases in viscosity, can make it hard to discharge glass into the canister and can also make it difficult to incorporate new batch materials into the melt.

Additionally, the formation of crystals like spinels: (Fe, Ni, Mn, Zn)$(Fe,Cr)_2O_4$ can lead to crystal accumulation at the bottom of a melter pool, since the density of spinel crystals (~5.2 g/mL)[26] is more than twice as high as that of typical borosilicate waste glass (~ 2.75 g/mL).[27] Spinel crystals were found to build up in the glass discharge riser of DWPF pilot scale melters during melter idling. This problem was mitigated at DWPF by adding heaters to the riser, lining it with Inconel® 690, and having a riser slope design that was not favorable towards crystal accumulation. Conversely, glass trapped in the riser at WTP is relatively cool and stagnant as opposed to glass in the bulk of the melter, which is fairly well mixed by thermal gradients created by convective currents and bubblers positioned near the bottom of the melter, Additionally, the narrow dimensions and slope of the WTP riser may assist in crystal accumulation and make it difficult to install heaters. Therefore, temperatures within the WTP riser have been projected to drop as low as 850 ℃ depending on the length of time between glass pours.[28] Because of the low temperatures and stagnant melts, the propensity for crystallization is high in the WTP riser. Moreover, because of the small diameter of the WTP riser and the recent proposal for using waste loadings that allow spinel crystals to form in the WTP melter, the WTP riser is more susceptible to becoming blocked with accumulated solids[13] than at DWPF where the riser is wider, heated, and waste loading is designed to prevent spinel crystallization in the melt. A blockage in the riser would prevent glass from being poured, thereby rendering the melter useless unless mitigation techniques or strategies are developed and implemented. Additionally, refractory-glass interactions[29], which may give rise to heterogeneous crystallization, are increased in the narrow WTP riser since the surface to volume ratio of the melt is high. It is also worth noting that even a small accumulation of crystals (<1 vol.%) can act as nucleation sites to govern the formation and/or growth of future crystals. Thus, in the narrow discharge riser, it is expected that spinels will continue to accumulate and grow in the same vicinity, thus increasing the likelihood of a clog.

Despite the many years of research on spinel crystallization and the many process control constraints at DWPF, a small fraction of crystals was once found in the lower bore of the riser of DWPF Melter #2 (shown in Figure 3-2[30]) due to a heat sink problem.[31] These crystalline deposits are shown in Figure 3-3 and Figure 3-4. The heat sink problem was eliminated by design of a heated bellows for the lower bore. Overall, the potential negative impacts of spinel crystallization have been severely reduced for DWPF because of the liquidus process constraints and historical processing that identified potential operation conditions to avoid during processing.

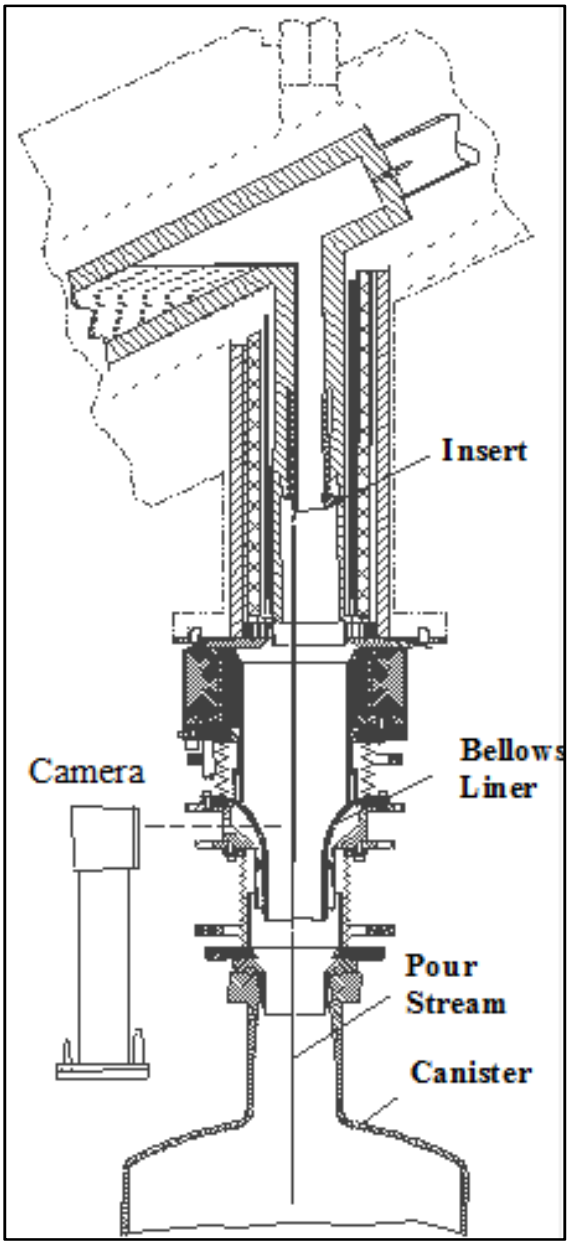

Figure 3-2. DWPF pour spout schematic showing the location of the upper bore (section above the insert), the insert, the pour stream, and the canister.[30]

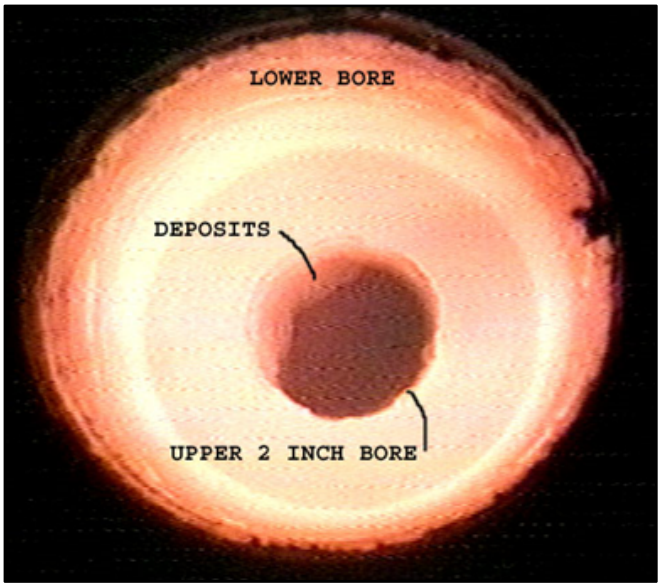

Figure 3-3. Region of the upper pour stream bore from which PC0031 sample was taken. Note deposits appear thicker on the glass pour side. This is not typical of normal operation.[31]

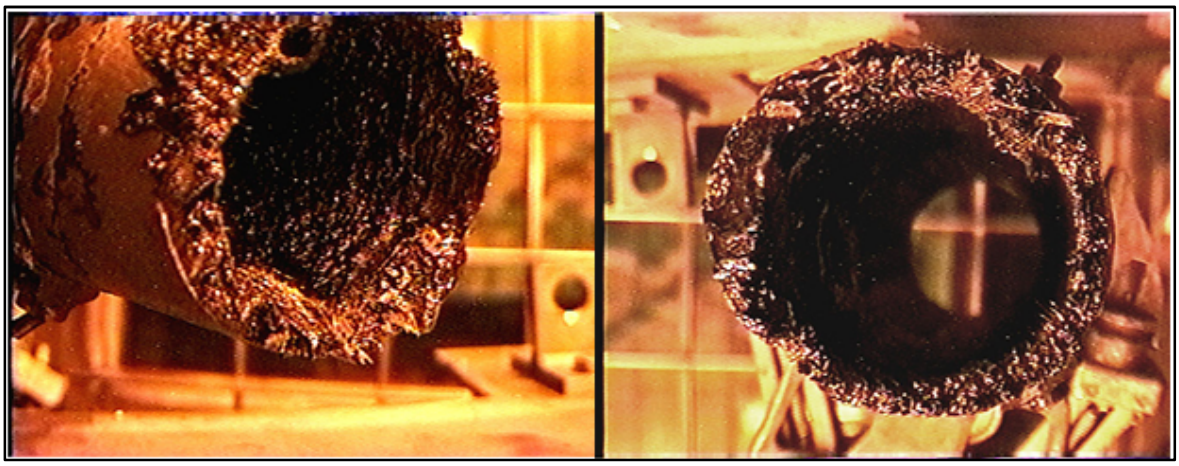

Figure 3-4. Region of the pour spout insert from which the PC0006 sample was taken. Note the heavy buildup of deposits. This is not the typical appearance of DWPF melter inserts.[31]

While spinel crystallization is most problematic if it were to occur inside a HLW melter, crystals like nepheline, which can form during slow cooling inside of a HLW canister, can be problematic once glass leaves the melter, because these crystals can weaken the glass network from which they formed by depleting certain glass-formers in the matrix and creating grain boundaries which can preferentially leach. This occurs, because nepheline formation removes three moles of glass-forming oxides (Al_2O_3 and $2SiO_2$) per each mole of Na_2O or K_2O. Importantly, not all Al, Si, Na, and K react to form nepheline. Although the removal of alkali metal oxides (fluxes) can increase glass durability, SiO_2 and Al_2O_3 are glass network formers, and their removal can result in a severe deterioration of a glass's chemical durability.[32]

Although, HLW components vary based upon how the waste was produced and blended, there exists the possibility for nepheline crystallization to occur in HLW glass since Al_2O_3 and Na_2O are common in many nuclear waste streams. While some Al and Na can be separated from HLW during pre-treatment

stages, this leads to increased costs of sludge processing operations as well as increased low-activity waste (LAW) disposal volumes, but is off-set by decreased HLW disposal volumes. Additionally, Na and Al have beneficial roles in glass processing. Sodium is a flux ion, which can lower the glass melting temperature. Additions of Al can often limit boron and silicon (liquid-liquid) phase separations, which can negatively impact chemical durability and make it difficult to predict using Equation 1.

A basic assumption in all glass dissolution models, as well as in all single phase mineral dissolution models, is that the solid being modeled is comprised of a single phase and so the durability response has only one source term. Therefore, phase separated glasses which are comprised of two immiscible glass phases, have two source terms and cannot be modeled in this fashion, since one phase is usually more soluble than the other and different radionuclides partition to the different immiscible phases. Thus the distribution of the radionuclides in the two glassy phases and the extent of phase separation would have to be known for every phase separated waste glass fabricated.

If crystals are present in a glass, crystals can create grain boundaries that can (1) selectively undergo accelerated dissolution while the crystals themselves may have a different dissolution response[33] or (2) have compositions not representative of the bulk glass.[34] To ensure that HLW glasses at DWPF are homogeneous, a minimum Al_2O_3 limit is applied. The effect of insufficient Al_2O_3 was first reported by French researchers[35] who determined that many glass durability models were non-linear, e.g., glasses had release rates far in excess of those predicted by most models, in regions corresponding to low Al_2O_3 and in excess of 15 wt.% B_2O_3. These results were independently reported by Jantzen, et al.[36] Homogeneous glass formulations, or formulations with only 1-2 wt.% crystals, are targeted for HLW in the U.S. at WTP. Crystals such as iron spinels have little impact on glass durability as they are themselves very durable and cause minimal grain boundary dissolution since the spinels and the glass are both isotropic.[37] However, for other phases such as nepheline, acmite, and lithium silicates that are less durable than iron spinels and not isotropic, the impact on glass durability from the crystal and the grain boundary can be pronounced[a]. This is especially true if the crystal sequesters radionuclides as this gives a secondary source term for radionuclide release. Therefore, durability testing must be performed to confirm that any crystallization that might occur during canister cooling or during glass composite material (GCM) formation has minimal impact.[38,39,40,41]This ensures that the last 3 terms in equation 1 are approximately zero and that the dissolution models do not represent mixed mechanisms.

Equation 1[42]

$$\sum Durability = \left(\underbrace{durability_{(homogenous)}}_{1st\ term} + \underbrace{durability_{(amorphous\ phase\ separation)}}_{2nd\ term} + \underbrace{durability_{(crystallization)}}_{3rd\ term} + \underbrace{durability_{(accelarted\ grain\ boundary}}_{4th\ term} \right)$$

Thus, the DWPF operates using a minimum Al_2O_3 constraint in conjunction with an upper alkali metal ($\sum$ = Li_2O, Na_2O, K_2O, Cs_2O) constraint to prevent the development of amorphous phase separation and/or non-predictable glass formulations.

The next section highlights several research topics related to spinel crystallization in HLW immobilization.

[a] Nepheline can be a liquidus phase but acmite and lithium silicates are subliquidus phases only found during cooling of HLW glasses under certain regimes.

4.0 Research Highlights of Spinel Crystallization in High-Level Waste Glass

This chapter highlights research on spinel crystallization as it occurs during HLW vitrification. It describes the details of the current liquidus temperature model used at the DWPF, highlights the role of quasicrystalline glass structure and thermodynamic octahedral site preference energies in predicting spinel formation, and gives details regarding the kinetics of spinel growth. In order to move away from the use of a T_L constraint and towards the processing of glasses with some volume percent of crystallization, understanding these factors is necessary in determining the effects of solid and gaseous inclusions on the glass melting process and its modeling

The spinels are a class of minerals with the general formula $A^{2+}B^{3+}{}_2O^{2-}{}_4$. Understanding spinel crystallization in HLW glass is a key issue for successful glass processing, namely, reducing the accumulation of solids in the melter while maximizing the waste loading to minimize disposal volume of the final waste form. Spinel is easily the most prominent crystalline phase formed from HLW during typical liquidus measurements at DWPF, with nepheline and other crystalline phases tending to only form during centerline canister cooled (CCC) heat treatments or time-temperature transformation (TTT) measurements, which assess the phase stability of HLW glass as a function of time and temperature. [14a]

The spinel phase that crystallizes from HLW melts is nominally $NiFe_2O_4$, which is an inverse $BABO_4$ spinel. In this structure the divalent ions (B = Mg^{2+}, Zn^{2+}, Fe^{2+}, Ni^{2+}) are in an octahedral coordination, while half of the Fe^{3+} are in tetrahedral coordination at the A lattice site, and the other half are in an octahedral coordination.[14a] Substitution of Cr^{3+}, Al^{3+}, and occasionally Ti^{3+} for Fe^{3+} can occur; however, aluminate, chromite, and $MnFe_2O_4$ spinels have a normal spinel structure in which all of the trivalent species prefer the octahedral sites and the Mn^{2+} occupies the A lattice site.[14a]Although spinel crystal formation in HLW glass does not negatively affect the chemical durability of the glass from which it formed[43], and thus does not make glass unacceptable for disposal in geologic repositories, the formation and accumulation of spinel crystals can negatively affect melter operations as described in detail in Section 2.

For glasses whose primary liquidus phase can vary greatly in composition and elemental substitution (like HLW glass), well-designed, compositionally dependent models capable of accurately predicting glass behavior can be difficult to develop. A unique model relevant to the complex nature of DWPF-type glass compositions was developed at SRNL by Jantzen and Brown[14] and is described herein. This semi-empirical model is currently incorporated in the DWPF Product Composition Control System (PCCS) in order to predict the spinel liquidus temperature as a function of glass composition while simultaneously evaluating the prediction relative to acceptability limits.[44] This is a spinel only liquidus model as spinel is always the primary liquidus phase in DWPF glasses.

In two papers by Jantzen and Brown[14], predictions of the spinel-nepheline liquidus are made on the basis of quasicrystalline concepts and a freezing point depression model. As a start, the authors compile the primary liquidus phase(s) for a large number of glasses that have been studied for HLW immobilization applications, and give a brief description of the glass chemistry as shown in
Table 4-1. In the majority of said glasses, spinel is the primary liquidus phase and nepheline precipitates at subliquidus temperatures. In glasses that have little or no iron and other transition metals, like the WTP LAW glasses, nepheline can be the primary liquidus phase. The composition of the spinels formed from HLW can be understood on the basis of the known crystallographic preferences of any ion for the spinel octahedral site , which is found to diminish in the following order: $Cr^{3+} > Ni^{2+} > Ti^{3+} > Fe^{2+} > Fe^{3+} > Mn^{2+}$.[26] Additionally, the preference of any ion for the spinel tetrahedral site is: $Zn^{2+} > Mn^{2+} > Fe^{3+} > Ga^{3+} > Co^{2+} > Mg^{2+} >$.[26] Thus, on the basis of spinel site preference it should not be surprising that $Ni(Cr,Fe)_2O_4$ is normally the primary phase that forms in HLW glass.

Next, the role of medium range order and quasicrystals in spinel forming melts is described. Borosilicate waste glasses and melts, like natural silicate glasses and melts, possess short-range order (SRO, radius of influence ~ 1.6 -3 Å) around a central atom.[5] Glasses also possess medium-range order (MRO), which encompasses second and third-neighbor environments around a central atom (radius of influence ~ 3 -6 Å).[5] The more highly ordered regions are referred to as quasicrystals, since they often have atomic arrangements that approach those of crystals. When the medium-range order in a glass or melt becomes enough like that of a crystalline phase then nucleation and crystal growth may occur.[5] The departure from melt to crystal usually involves an increase in the cation coordination number and a decrease in the distance between cations and oxide ligands, as shown in equation 2.[45]

$$\text{Melt}_{\text{cation}} \xrightarrow{\textit{increased coordination or decreased } M-O \textit{ distance}} \text{Crystalline}_{\text{cation}} \quad \textbf{(2)}$$

Table 4-1. Primary Liquidus Phases Formed at 24 h in Simulated Waste Glasses

Number of glasses studied	Waste type	Number of glasses crystallized and identification of primary liquidus phase (s)	Glass chemistry
51	DWPF—average, high Al_2O_3, high Fe_2O_3	50 Spinel 1 Nepheline	Frits 165, 131 for sludge only flowsheet, Frits 200, 202 for coupled waste flowsheet, DWPF startup Frit
1	None	1 Tridymite+unknown	Pure Frit 165
2	DWPF—average	2 Spinel	2.8 wt% UO_2, 0.26 wt% ThO_2, noble metals, Frit 165, $Fe^{2+}/\Sigma Fe = 0.01$ to 0.21 ± 0.02
1	DWPF—high Al_2O_3	1 Spinel+nepheline	0.91 wt% UO_2, 1.08 wt% ThO_2, noble metals, Frit 131, a high Na_2O frit with TiO_2 that may help nucleate nepheline.
1	DWPF—high Al_2O_3	1 Spinel	0.91 wt% UO_2, 1.08 wt% ThO_2, Frit 165, noble metals
2	DWPF—average	2 Spinel	2.27 wt% UO_2, 0.29 wt%ThO_2, Frits 131/165, noble metals
2	DWPF—high Fe_2O_3	2 Spinel	4.15 wt% UO_2, 0.03 wt%ThO_2, Frits 131/165, noble metals
1	DWPF—high Al_2O_3	1 Nepheline	Frit 411, a high Na_2O frit
1	DWPF—high Fe_2O_3	1 Spinel	Frit 411, frit higher in Li_2O and lower Na_2O than Frit 211
1	DWPF—high Fe_2O_3	1 Spinel	Frit 211, frit contains more Na_2O and less Li_2O than Frit 411
7	DWPF—average, high Al_2O_3, high Fe_2O_3	7 Spinel	Waste Compliance Plan Glasses (Frit 200+202), noble metals
24	WVNS	24 Spinel	Simulated with high ZrO_2, non-radioactive
3	WVNS	3 Spinel	0.47 wt% UO_2, 3.57 wt%ThO_2, noble metals, $Fe^{2+}/\Sigma Fe = 0.1$
33	Hanford HLW tank waste—high Fe_2O_3	33 Spinel	SP glass matrix, noble metals
36	Hanford TRU waste—high ZrO_2	36 $ZrSiO_4$, ZrO_2, CeO_2	TRU glass matrix
20	Hanford HLW—high Na_2O waste	4 Nepheline; 2 Other silicates; 14 Spinel	NP glass matrix; evidence that nepheline grew on spinel crystals
51	DWPF—average, DWPF—high Fe_2O_3, DWPF—high Fe_2O_3	44 Spinel 7 Clinopyroxene	SG glass matrix, contained noble metals, some glasses contained UO_2
1	Hanford HLW Envelope D waste	1 Nepheline+Spinel	Contained noble metals, low SiO_2, high Al_2O_3, high Na_2O, and 1.87 wt% UO_2
23	Hanford HLW	11 Spinel; 3 zirconates; 2 Ca-silicate, 2 olivine, 2 SiO_2, 1 othopyroxene	CVS-I, two glasses never crystallized
100	Hanford HLW	42 Spinel; 4 SiO_2, 14 zirconates; 4 Ca-silicate; 2 olivine; 3 othopyroxene; 10 clino-pyroxene; 6 nepheline; 4 Cr_2O_3; 5 $LiSiO_3$	CVS-II, contained noble metals, two glasses contained UO_2 and were not measured, four glasses did not crystallize

When transition metal ions leave sites of irregular coordination in the melt for regular octahedrally coordinated sites in a crystalline structure, they gain energy due to the shortening of interatomic distances.[46] This energy gained is called the Octahedral Site Preference Energy (OSPE) and is documented for several cations.[46]

Understanding the role of the OSPE and the relative stability of spinel forming quasicrystals in the melt, versus the stability of the metal cations in crystalline spinels, is described as one method in which HLW crystallization can be predicted. In essence, the quasicrystals identified in the melt are argued as the basis of what crystals will form at the liquidus temperature. The formation of these species is a complex balance between which ions have a greater preference for a particular coordination site. In order to study the role of each transition metal cation in a complex (> 15 component) system, glasses were made from an average DWPF waste and borosilicate frit (F202). The transition metals: Ni^{2+}, Fe^{2+}, Mn^{2+}, and Mg^{2+} were added separately to glasses containing either: Fe^{3+}, Fe^{3+} and Al^{3+}, Cr^{3+}, Cr^{3+} and Al^{3+}, or Al^{3+}. This one-at-time method allowed for the determination of each divalent cations reactivity with the various trivalent cations found in the melt. The results of this study are summarized in Table 4-2.[14a]

Table 4-2. Spinel Solid Solutions Formed in Limited Component Waste Glasses Melted at 1050 ℃ and 1150 ℃

Divalent cation present	Fe^{3+}	Fe^{3+} and Al^{3+}	Cr^{3+}	Cr^{3+} and Al^{3+}	Al^{3+}
Melt Temperature of 1150°C					
Ni^{2+}	Amorphous	$NiFe_2O_4$	$Cr_2O_3+SiO_2$	$NiCr_2O_4+Cr_2O_3$	Amorphous
Fe^{2+}	Amorphous	Fe_3O_4[†]	(Oxidized and reduced) $Cr_2O_3+SiO_2$ Crist[‡]	(Oxidized and reduced) Cr_2O_3[‡]	Amorphous[§]
Mn^{2+}	Amorphous	$Fe_2O_3+SiO_2$ (Qtz.)	Cr_2O_3	$MnCr_2O_4+Cr_2O_3$	Amorphous
Mg^{2+}	$MgFe_2O_4$-Fe_3O_4 Solid solution (poorly crystallized)	Fe_2O_3	$Cr_2O_3+SiO_2$ Crist.	Cr_2O_3	Amorphous
Melt Temperature of 1050°C					
Ni^{2+}	$NiFe_2O_4$	$NiFe_2O_4$	$Cr_2O_3+SiO_2$ (Tridy+Crist+Qtz)	Cr_2O_3	SiO_2
Fe^{2+}	Fe_3O_4[¶]	Fe_3O_4[†]	$LiCr(SiO_3)_2$ (oxidized) Cr_2O_3 $+LiCr(SiO_3)_2+SiO_2$ Crist (reduced) Cr_2O_3+ $LiCr(SiO_3)_2$ $+SiO_2$ (Crist)[‡]	(oxidized) $Cr_2O_3+LiCr(SiO_3)_2$ (reduced)Cr_2O_3[‡]	SiO_2[§]
Mn^{2+}	Amorphous	Did not melt	Cr_2O_3	$Mn_{1.5}Cr_{1.5}O_4+Cr_2O_3$	SiO_2
Mg^{2+}	Amorphous	Fe_2O_3	Cr_2O_3	Cr_2O_3	SiO_2

Through glass analysis via Scanning Electron Microscopy (SEM) with Energy Dispersive X-ray Spectroscopy (EDS) and powder X-ray Diffraction (XRD), the prominent spinel melt precursors were ultimately defined as $Ni_{0.5}(Al_{0.5}Cr_{0.5})O_2$ and $2(K,Na)AlO_2$ quasicrystals, while the nepheline precursors (at the liquidus) were (K, Na, Li)FeO_2. The OSPE was shown to govern the exchange equilibria between the quasicrystalline species in the melt and the crystalline species at the liquidus. The experimental data in this study indicated that the OSPE for spinel forming cations in complex multicomponent nuclear waste glasses is $Ni^{2+} \sim Fe^{2+} > Mg^{2+} > Mn^{2+}$, which is in agreement with the sequences determined in previous studies in simpler systems[26]

In order to develop a robust liquidus temperature model, Jantzen and Brown go on to use a freezing point approach based on calculation of the quasicrystalline melt precursors. The model, described herein, adequately describes the liquidus temperature in a variety of HLW glasses, and has been used as a process

control at the DWPF since Melter #2 was installed in 2003.[47] The model is developed on the approximation that the phase diagram of borosilicate waste glass is similar in composition to the geochemical basalt quaternary: Fe_2O_3-Al_2O_3-SiO_2-Na_2O and the reduced iron: Fe_3O_4-Al_2O_3-SiO_2-Na_2O system on a borate-free basis; however, since borate phases do not crystallize at the liquidus in HLW, the two systems can be compared rather well. This quaternary shown in Figure 4-1 also shows that a pseudobinary phase diagram between, transition metal ferrite-rich spinels and nepheline falls in the basalt quaternary.

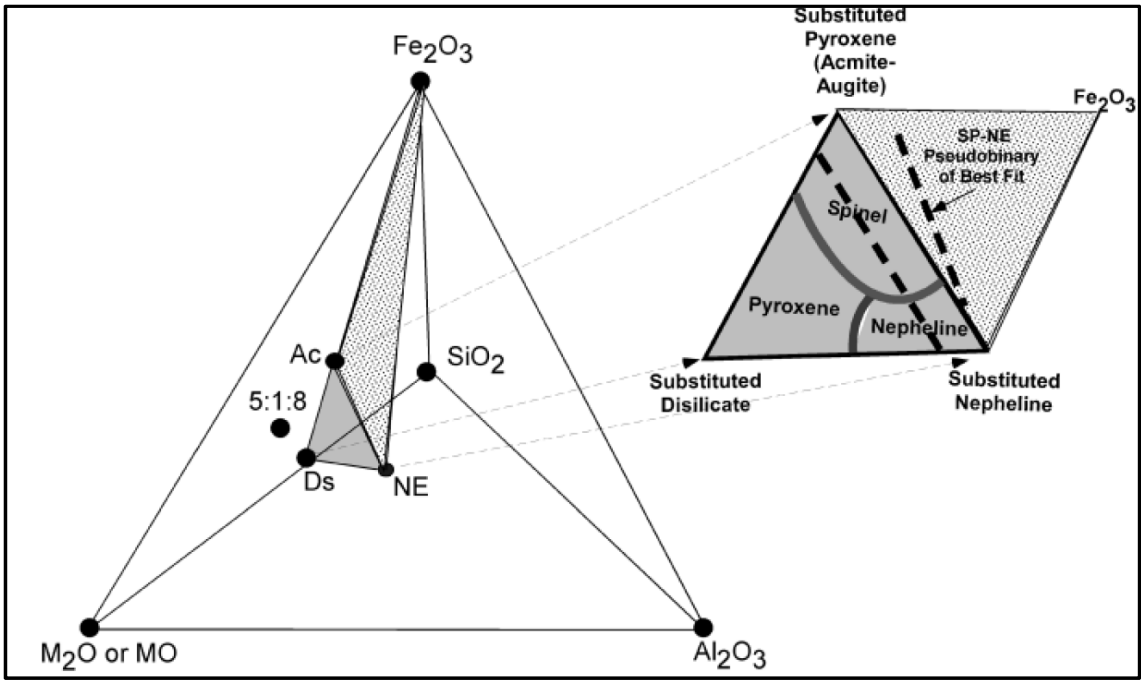

Figure 4-1. Quaternary system Fe_2O_3-Al_2O_3-SiO_2-M_2O(M = Na in basalt glass) showing the position of the ternary system involving acmite (Ac), nepheline (NE), and disilicate (Ds). Jantzen and Brown used this as a starting point for modeling the spinel-liquidus temperature in HLW glass.[14b]

It's noted, that the addition of a nepheline-type quasilattice to the primary phase [P] pyroxene (acmite) quasilattice (the phase from which spinel precipitates as acmite melts incongruently to spinel and liquid), results in a lowering of the system freezing point congruent with a change in the solubility of the melt.[48] By definition, this requires the chemical potentials of the pure crystalline primary phase and the primary phase in the liquid (melt) to be equal at any point along the freezing point curve.[48] The chemical potentials are related to the activity of the primary phase, which can be correlated to the liquidus temperature by the relationship:

$$-Rln\,[a(P_l)] \approx \Delta H_{fus,P}(T_P^*)[\frac{1}{T_L} - \frac{1}{T_P^*}] \quad \textbf{(3)}$$

Where $a(P_l)$ represents the activity of P, the primary crystalline phase in the liquid (melt), R is the ideal gas constant, $\Delta H_{fus,P}$ is the enthalpy of fusion for P, T_L is the liquidus temperature, and T_P^* is the temperature of P in the melt. Assuming an ideal solution, the molar concentration of P can be substituted for the activity; however, measuring the molar concentration or activity of P can be difficult in a complex liquid system with multiple crystalline phases forming, and thus it must be approximated.

By making several assumptions, the authors conclude that the activity of the primary phase can be approximated by:

$$a(P_{(l)}) \approx K_P(M_2)^a(M_1)^b(M_T)^c \quad \textbf{(4)}$$

Where K_P is the equilibrium constant for pyroxene, the superscripts are based on stoichiometric ratios between M ions (which are difficult to estimate due to ion vacancies), and the M terms represent the mole fraction of cations occupying a specific site in the pyroxene formula, which is generally:

$$(M_2^{VI\text{-}VIII})_2(O)\cdot(M_1^{VI})_2O_3\cdot 4(M_T^{IV})O_2 \quad \textbf{(5)}$$

(Superscripts represent coordination states of the cations in a pyroxene or acmite-like structure)

Based on the known role of each element in crystalline pyroxene (acmite) and nepheline, a table of proposed cation substitutions for waste glass quasicrystalline complexes is shown in Table 4-3.

Table 4-3. Proposed Cation Substitutions for Waste Glass Quasicrystalline Complexes. (CN is coordination number).

Pyroxene-like Precursor			Nepheline-like Precursor	
MT (IV CN)	M1 (VI CN)	M2 (VI–VIII CN)	T1 (IV CN)	N1 (VIII–IX CN)
Si^{4+}			Si^{4+}	
Al^{3+}	Al^{3+}		Al^{3+}	
Fe^{3+}	Fe^{3+}		Fe^{3+}	
	Ti^{4+}		Ti^{4+}	
	Cr^{3+}			
	Zr^{4+}			
	Ni^{2+}	Ni^{2+}		
	Mg^{2+}	Mg^{2+}		
	Mn^{2+}	Mn^{2+}		
		Ca^{2+}		
		K^+		K^+
		Li^+		Li^+
		Na^+		Na^+

The M terms in equation 4 can be directly calculated using the mole fraction ($\phi_{i,j}$) of each species (j) associated with a particular (i) site and the total moles of that species (Z_j) per 100 g of glass. For example, Table 4-3 shows that Si^{4+}, Al^{3+}, and Fe^{3+}, are possible MT site cations in pyroxene-like precursors. These ions are produced in the melt from SiO_2, Al_2O_3, and Fe_2O_3 respectively, thus:

$$\Sigma_{MT} = \phi_{T,SiO_2}Z_{SiO_2} + \phi_{T,Al_2O_3}Z_{Al_2O_3} + \phi_{T,Fe_2O_3}Z_{Fe_2O_3} \quad \textbf{(6)}$$

Similar equations are used for spinel M1 and M2 sites, as well as T1 and N1 sites in nepheline.
Thus the appropriate mole fraction of MT is:

$$\text{MT} = [(\text{MT})O_{2(l)}] = \frac{\Sigma M2}{\Sigma} \quad \text{where } \Sigma = \Sigma_{MT} + \Sigma_{M1} + \Sigma_{M2} + \Sigma_{T1} + \Sigma_{N1} \quad \textbf{(7)}$$

Thus, for pyroxene crystallization, the liquidus temperature can be obtained by modification of equation 3:

$$\left(\frac{1}{T_L}\right) \approx -\frac{R}{\Delta H_{fus,P}(T_P^*)}\ln\{M_2^a M_1^b M_T^c\} + \{\left(\frac{1}{T_P^*}\right) - \frac{Rln(K_P)}{\Delta H_{fus,P}(T_P^*)}\} \quad \textbf{(8)}$$

Since the properties assumed to control crystallization (e.g. fusion enthalpy [ΔH_{fus}], melt temperature [T_P^*], etc.) of the melt phase complexes are unavailable, the properties were estimated from the least-squares fitting results of empirically obtained liquidus temperature data measured on DWPF representative compositions. Additionally, because there are no data on exactly how the cations distribute in molten glass, a trial-and-error method was used to estimate cation distributions on a large number of glass compositions until Eq. 8 yielded an acceptable fit to the experimental liquidus data as shown in Figure 4-2. The estimated cation distributions are shown in
Table 4-4.

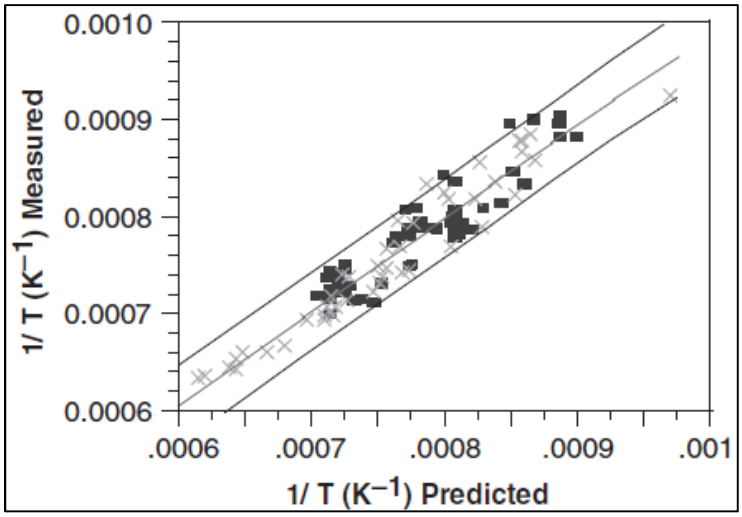

Figure 4-2. The relationship between the reciprocal liquidus temperature and the quasicrystalline composition terms for acmite (spinel) for 105 designed (X) and extreme (▬) glass data are fit to Eq. 8 at the 95% confidence interval.

Table 4-4. Cation distribution in waste glass just before crystallization

	Pyroxene-like Precursors			Nepheline-like Precursors		
	M2	M1	MT	N1	T1	SUM
Al_2O_3	0	0.0607	0.9393	0	0	1.0000
B_2O_3	0	0	0	0	0	0.0000
CaO	0.029	0	0	0	0	0.0290
Cr_2O_3	0	0.9202	0	0	0	0.9202
Fe_2O_3	0	0.1079	0.0193	0	0.6094	0.7366
K_2O	0.3041	0	0	0.1049	0	0.4090
Li_2O	0.1745	0	0	0.1068	0	0.2813
MgO	0.0167	0.0223	0	0	0	0.0390
MnO	0.994	0.00603	0	0	0	1.0000
Na_2O	0.1671	0	0	0.2518	0	0.4189
NiO	0	0.1079	0	0	0	0.1079
SiO_2	0	0	0.0193	0	0.0133	0.0326
TiO_2	0	0.0568	0	0	0.5667	0.6235
U_3O_8	0	0	0	0	0	0.0000
ZrO_2	0	0.0458	0	0	0	0.0458

The equation describing the liquidus temperature of spinel forming glass was thus simplified to:

$$T_L(°C)_{spinel} = \{aln(M2) + bln(M1) + cln(M_T) + d\}^{-1} - 273 \quad \textbf{(9)}$$

Where a = -0.000260, b = -0.000566, c = -0.000153, and d = -0.00144. A similar equation is used to describe the nepheline liquidus temperature:

$$T_L(°C)_{nepheline} = \{aln(N1) + bln(T1) + c\} - 273 \quad \textbf{(10)}$$

Where a = -0.0001498, b = +0.0005328, and c = +0.001757. Both the spinel and nepheline equations (9 and 10 respectively) yielded acceptable fits to experimentally determined liquidus temperatures for a variety of crystal forming glasses, as shown in Figure 4-3.

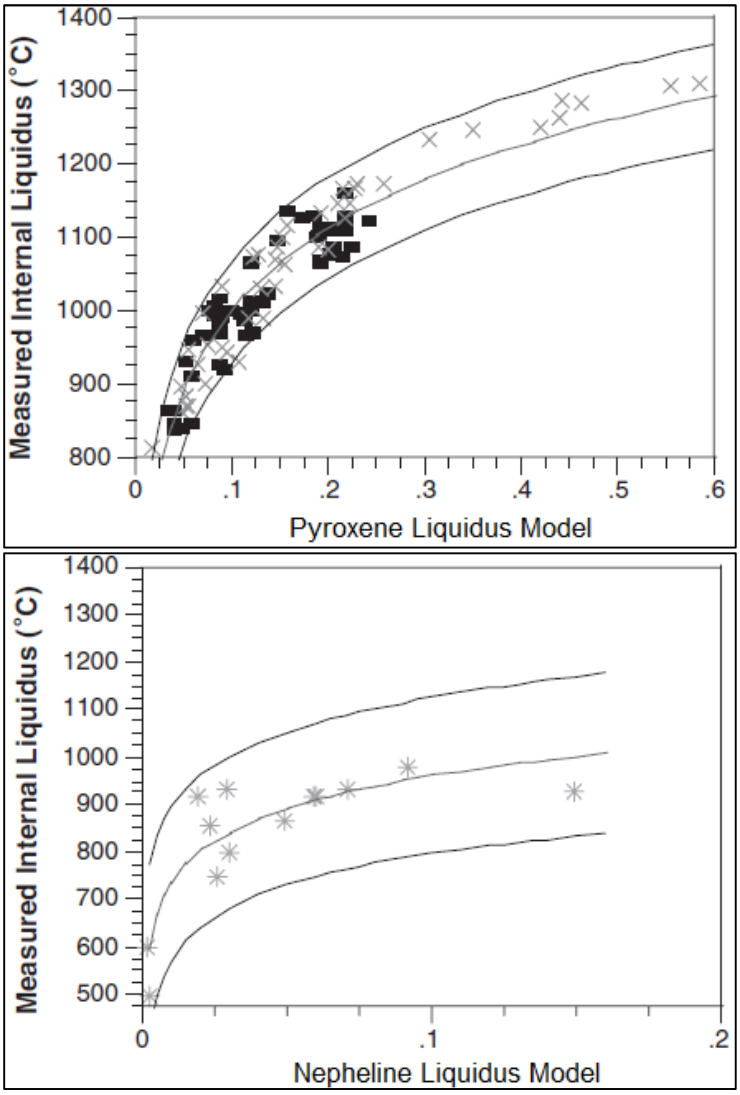

Figure 4-3. The pyroxene (spinel) and nepheline liquidus equations (Eqs. 9 and 10 respectively) are fit to the measured liquidus temperature of a variety of glass compositions. The equations yield acceptable fits, although there is more error associated with the nepheline liquidus than the spinel liquidus; however, this is attributed to significantly less nepheline liquidus data being used in the fit.

Using the experimental data and equations 9 and 10, the pseudobinary diagram between spinel and nepheline was expressed in terms of the pyroxene and nepheline precursor compositions (mol %). These results are shown in Figure 4-4. The spinel-nepheline pseudobinary was validated using data from TTT measurements on a variety of spinel and nepheline forming glasses, where it was noted that nepheline can form on the liquidus in the absence of a significant amount of iron, but if one is on the spinel side of the eutectic in Figure 4-4 then nepheline forms at subsolidus temperatures as glass cools in the disposal canister.

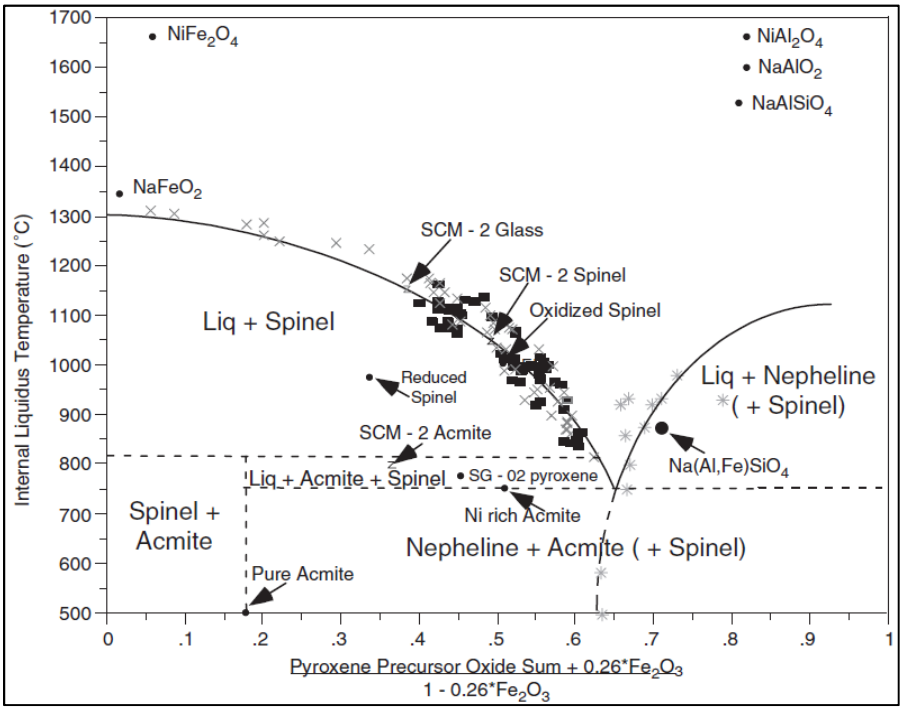

Figure 4-4. Pseudobinary phase diagram between acmite and nepheline expressed in terms of the pyroxene and nepheline precursor compositions (unnormalized mol %). The liquidus curves were generated by fits to the measured liquidus data with Eqs. 8 and 9.

Hrma et al.[4b] and Mika et al.[49] have performed analyses that examined the liquidus temperature of HLW borosilicate glasses with a spinel primary phase as a function of component additions to the glass batches. About half of this data was used in development of the liquidus temperature model described above. The T_L values in these studies ranged from 859 to 1310 °C. T_L was measured on 2.5 g samples that were heated in a "low to high temperature fashion" and were checked for the presence of crystals by optical microscopy, while the crystalline composition was determined using XRD and EDS measurements. When the difference in temperature between heat-treated glass samples with and without crystals was < 10 °C, the T_L value within this interval was estimated according to the size, shape, and numbers of crystals in the sample.

The primary crystallization phase in 44 glasses was spinel and was clinopyroxene in 7 glasses. The Cr content in spinel was found to decrease with increasing liquidus temperature and was higher at the interior of crystals than on the surface, indicating that just below T_L, Cr_2O_3 reacts with NiO and Fe_2O_3 forming a solid solution of nichromite ($NiCr_2O_4$), chromite ($FeCr_2O_4$) and magnetite (Fe_3O_4). Importantly, these reactions are in excellent agreement with the OSPE described above. At lower temperatures, spinel is increasingly enriched in trevorite ($NiFe_2O_4$) and magnetite (Fe_3O_4) as evidenced by EDS analyses, which

showed that Ni and Fe were major components of spinels formed at low temperatures. Additionally, clinopyroxene did not appear in glasses with <50 mass % SiO_2.

According to their effects on T_L, the glass components were arranged into four groups: (Cr_2O_3, NiO) >> (MgO, TiO_2, Al_2O_3, Fe_2O_3) > (U_3O_8, MnO, CaO, B_2O_3, SiO_2) > (K_2O, Li_2O, Na_2O), which is in fine agreement with the OSPE described by Jantzen et al.[14a] Components in the first group (Cr_2O_3, NiO) strongly increase T_L. Replacing 1 mass % SiO_2 with 1 mass % Cr_2O_3 results in a deviation in the T_L of ~ 200 ℃/mass %. Nickel oxide also strongly increases T_L by ~ 80 ℃/mass %. Components in the second group (MgO, TiO_2, Al_2O_3, Fe_2O_3) moderately increase T_L by ~ 17 to 44 ℃/mass %. Components in the third group have little effect on T_L (< 10 ℃ /mass %). Components in the fourth group, as expected (since the alkali metals are common fluxes), decrease T_L by 18 to 26 ℃/mass%.

In addition to the complexities and challenges faced in developing a robust liquidus temperature model for HLW, the behavior of spinel crystals in glass, specifically, the rate of growth, dissolution, and settling, is subjected to intricate thermodynamic and hydrodynamic conditions.[20, 50] To move away from the use of a T_L constraint and towards the potential processing of glasses with some volume percent of crystallization, understanding these factors is necessary in determining the effects of solid and gaseous inclusions on the glass melting process and its modeling

The kinetics of the growth and dissolution of spinel crystals were studied by Alton et al. using a simplified HLW glass. [50e] Measurements were performed over a range of temperatures that are present in a HLW melter. In this study, the Hickson-Crowell equation, which is based on Fick's first law of diffusion, is shown to be adequate at predicting the kinetics of spinel crystal growth in glass when the crystals move through the melt at a constant relative velocity for a sufficiently long time so that a steady state is established. This steady state occurs during the later stages in growth when the dense crystalline particles begin to descend at a constant velocity; however, it is worth noting that glass at DWPF is moved using a bubbler, which may prevent a steady state from occurring. WTP will also utilize bubblers in the melter. Importantly, the generated bubbles can act as nucleation sites, thereby enhancing nucleation and affecting the kinetics of crystallization.

The experiments were conducted with a simplified HLW glass (MS-7 glass) that contained 11 major glass species, including the common spinel forming components: Fe_2O_3, NiO, Cr_2O_3, and MnO. Importantly, the HLW glass used in this study did not contain insoluble noble metals, which are ever-present in waste glass, and which act as nucleation sites that can alter the crystallization kinetics. Thin sectioned samples polished with Al_2O_3 micro polish were prepared and the crystal size was measured by optical microscopy using image-analysis software (Clemex 3.0). The number density of spinel crystals (V_s/a^3) (where a^3 is the effective crystal size and V is volume of the spinels) was determined in powdered glass by quantitative XRD using an intensity standard, and was checked directly by optically counting the number of crystals in a measured glass volume.

By measuring T_L, the temperature at which the glass was held in the furnace during an isothermal heat-treatment (T), and the spinel mass fraction at equilibrium (C_0), it was shown that one can determine the maximum spinel mass fraction (C_{max}) that can form in a glass by performing a least-squares fit to equation 11, as shown in Figure 4-5. B_L is a temperature-independent fitting parameter representing the rate of change of C_o at $T = T_L$

$$C_0 = C_{max}\left\{1 - exp\left[-B_L\left(\frac{1}{T} - \frac{1}{T_L}\right)\right]\right\} \quad \textbf{(11)}$$

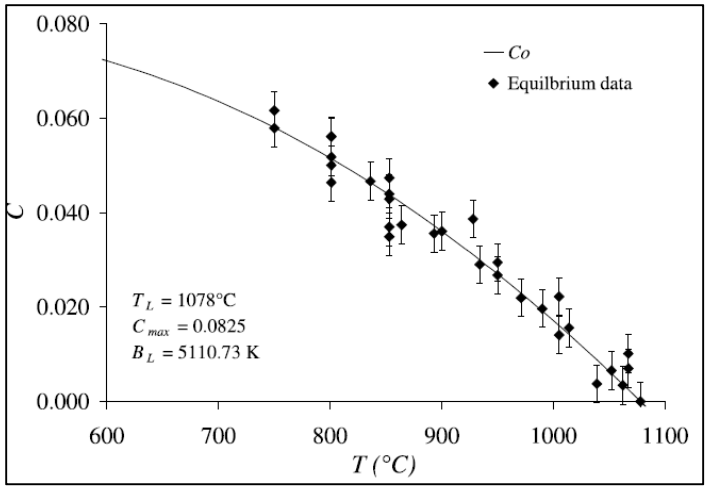

Figure 4-5. The equilibrium concentration (mass fraction) of spinel in simplified HLW glass versus temperature.

It was also demonstrated that crystal growth as a function of time is approximately linear except for the initial growth period (first 20 minutes) when growth is very rapid. This was demonstrated during isothermal heat-treatments, where the size of the formed crystals was monitored as a function time, as shown in Figure 4-6. The slope of the line in this plot gives the linear growth rate at a particular temperature; therefore, performing isothermal measurements at different temperatures allows for the determination of the temperature at which the crystal growth rate is the greatest, as shown in Table 4-5.These results indicate that the spinel growth rate is clearly highest around 800 ℃. There was some discontinuity in the growth rates between 800 ℃ and 820 ℃, as shown in Figure 4-7, which was attributed to the spinels changing crystal morphology from octahedral "stars" (T ≤ 820 ℃) to cubes (T > 820 ℃). Upon critical evaluation using the pseudobinary in Figure 4-4 these stars may also be ascribed to acmite as acmite melts incongruently to spinel and vice versa. The SEM images of these two spinel morphologies are shown in Figure 4-8.

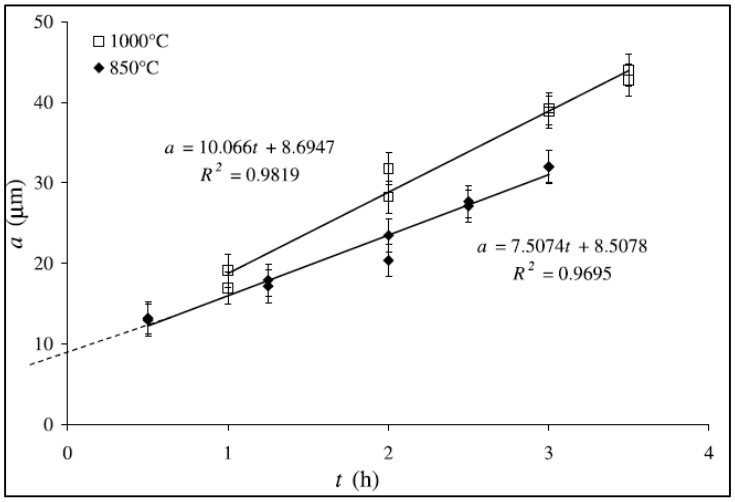

Figure 4-6. The size of growing crystals (a) versus the time the samples were held at 850 and 1000 ℃.

Table 4-5. Growth rates of spinel crystals in a simplified HLW glass.

Temperature (°C)	Linear growth rate (μm/h)
750	9.43
800	21.90
850	7.51
900	7.30
950	11.40
1000	10.07
1010	5.20
1050	9.54

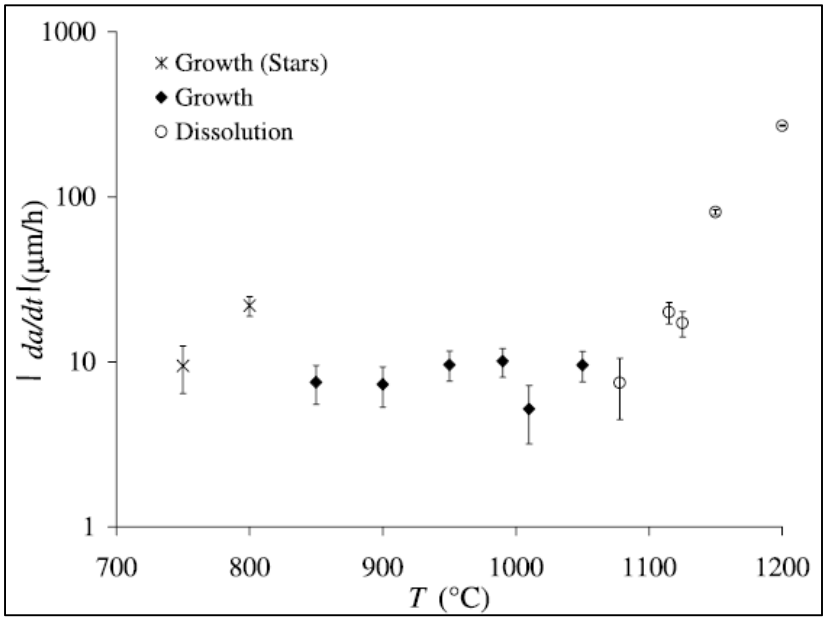

Figure 4-7. Steady-state rates of crystal growth. The discontinuity observed between 800 ℃ and 820 ℃ is attributed to the spinel transformation from a cubic to star-like morphology.

The size of the spinel crystals found at equilibrium is expressed by:

$$a_0 = \left(\frac{C_0 \rho_g}{n_s \rho_s}\right)^{1/3} \quad \textbf{(12)}$$

Where ρ_g and ρ_s are the glass and spinel densities respectively, n_s is the measured crystal-number density determined as $n_s = V_s/a^3$, and once again C_0 is the spinel mass fraction at equilibrium. Using the measured n_s and calculated a_0, one can perform a fit to $\frac{a}{a_0} = 2n_s a_0^2 k_H t$. The slope of this line forced through the origin (since the very initial state of growth-dissolution is disregarded) is taken as k_H, which is the mass transfer coefficient of the spinel crystals in units of m/s. The parameters: a_0, n_s, and k_H for both growth and dissolution of spinels at various temperatures are shown in Table 4-6.

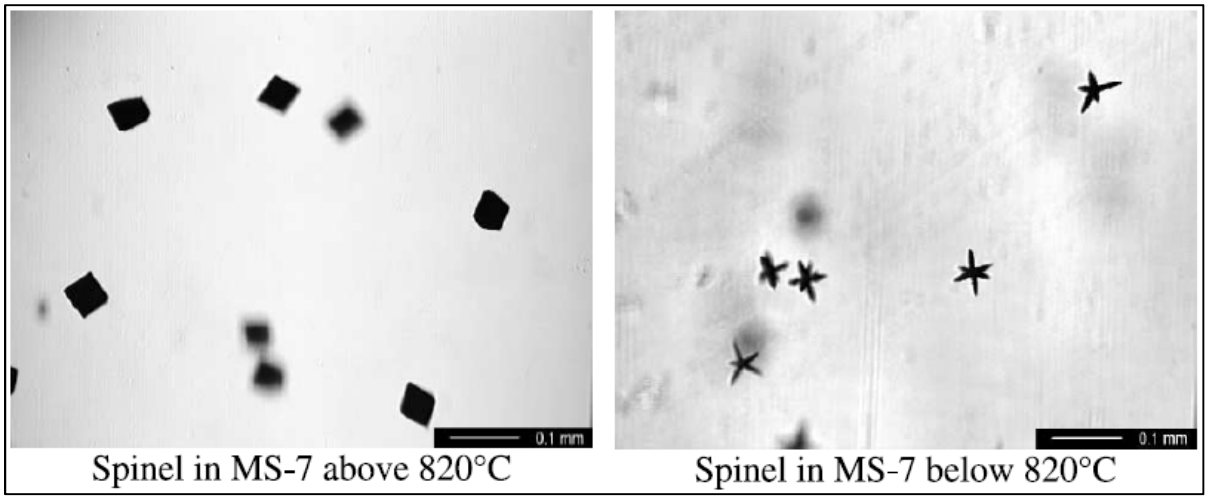

Figure 4-8. Cubic spinel crystals formed above 820 ℃ (left) and star-like spinel crystals (possibly acmite) formed below 820 ℃ (right).

Table 4-6. Parameters for spinel growth and dissolution data, where a_0 is the size of the spinel crystals found at equilibrium, n_s is the crystal number density, and k_H is the mass transfer coefficient, which relates the mass transfer rate, transfer area, and concentration change between phases.

Temperature (°C)	a_0 (m)	n_s (m^{-3})	k_H (m/s)
Growth			
850	6.51×10^{-5}	8.33×10^{10}	6.94×10^{-8}
900	7.28×10^{-5}	4.84×10^{10}	7.62×10^{-8}
950	7.92×10^{-5}	2.82×10^{10}	1.33×10^{-7}
990	8.15×10^{-5}	1.83×10^{10}	1.93×10^{-7}
1010	8.08×10^{-5}	1.47×10^{10}	1.73×10^{-7}
1050	7.01×10^{-5}	9.56×10^{-9}	5.85×10^{-7}
Dissolution			
1078	0.00×10^{-5}	4.84×10^{10}	2.84×10^{-7}
1115	-4.54×10^{-5}	4.84×10^{10}	3.96×10^{-7}
1125	-4.93×10^{-5}	4.84×10^{10}	3.22×10^{-7}
1150	-5.71×10^{-5}	4.84×10^{10}	9.35×10^{-7}
1200	-6.88×10^{-5}	4.84×10^{10}	1.81×10^{-6}
1200	-6.88×10^{-5}	4.84×10^{10}	2.75×10^{-6}

Although the Hixson-Crowell equation is capable of describing the kinetics of crystal growth and dissolution during a steady-state, which occurs during the later stages in growth when the dense crystalline particles begin to descend at a constant velocity (as shown above), the equation is unable to properly describe the early stages of growth and dissolution and is also unlikely to describe heterogeneous nucleation at insoluble noble metal sites. In order to elucidate the kinetics of crystallization when the crystals are too small to move with a velocity capable of affecting the concentration distribution around them, or at low temperatures when viscosity is high ($\eta > 10^6$ Pa s) and crystals aren't moving much

relative to their surroundings, Alton et al.[51] use the Kolmogorov-Mehl-Johnson-Avrami (KJMA) equation (a homogenous crystallization kinetic equation):

$$\frac{C_0 - C}{C_0 - C_i} = \exp[-(k_A t)^n] \quad \textbf{(13)}$$

where, C is the mass fraction of solid spinel in glass, C_0 is once again the mass fraction of solid spinel at equilibrium, C_i is the initial mass fraction of solid spinel in glass, t is time, k_A is the Avrami rate coefficient, and n is the Avrami exponent. In non-equilibrium conditions the kinetics are adequately described using Eq. 13 as shown in Figure 4-9.

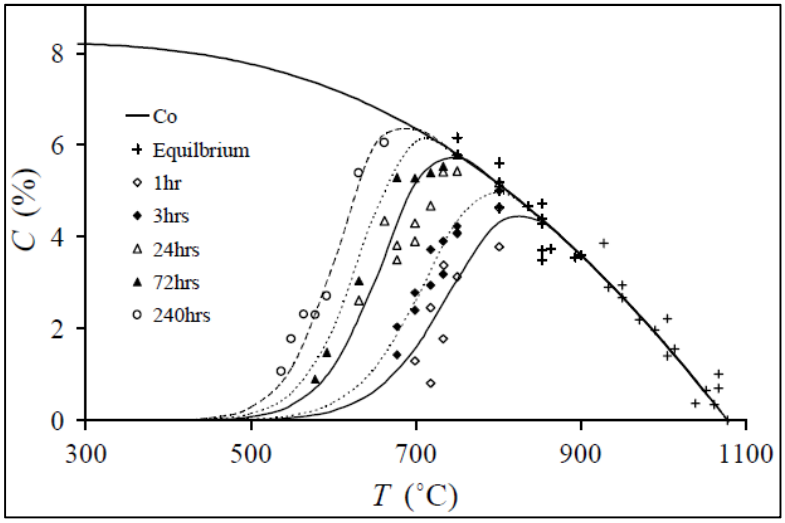

Figure 4-9. Spinel mass fraction in glass as a function of time and temperature. The solid and dashed lines, below the C_0 curve (calculated using Eq. 11), are fits to the KJMA equation (Eq. 13).

The crystal size growth can be described using:

$$a = a_0(k_A t)^{n/3} \quad \textbf{(14)}$$

where a is the spinel crystal size and a_0 (the crystal size at equilibrium) is determined by $a_0 = \left(\frac{C_0 \rho_g}{n_s \rho_s}\right)^{1/3}$ using measured n_s values. As shown in Figure 4-10, this equation yields a satisfactory fit to the experimental data when t is small, i.e. the very initial stages of crystal growth, while the Hixson-Crowell model is suitable for describing the later stages of growth.

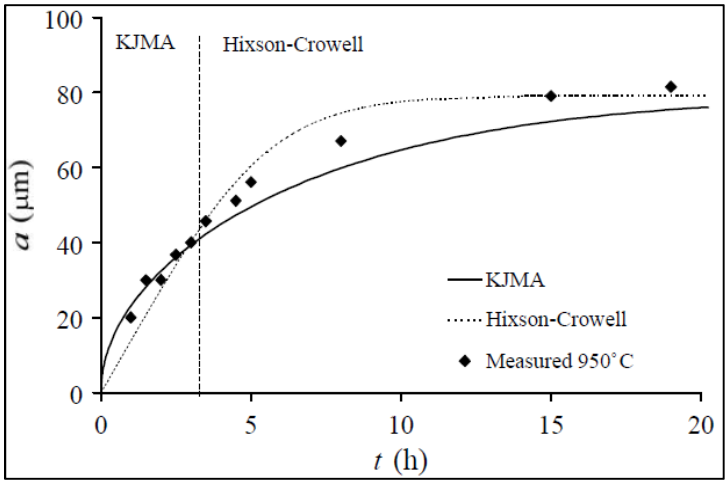

Figure 4-10. The crystal size (a) as a function of the time MS-7 glass spent at 950 ℃. At t < 4h the data are sufficiently described using the KJMA model. At t > 4h the KJMA model underestimates the crystal size and the Hixson-Crowell model is more suited once the settling motion of crystals is fully established.

The development of mathematical models that describe the rate at which spinel crystals grow, dissolve, and settle in a simplified HLW glass is of fundamental theoretical importance, and provides a path towards better understanding and modeling how spinel crystals might form and stay buoyant in a melter during vitrification of HLW.

In addition to modeling spinel crystal growth in simplified HLW glass, Hrma et al. [51] also show that the crystal number density (n_s) in MS-7 glass is significantly increased by the presence of nucleation agents, thus confirming a result that was originally reported in 1986.[19] Additionally, there is little temperature dependence of n_s when nucleation agents are present as opposed to when nucleation agents are absent as shown in Figure 4-11. It was also shown that Cr and Co increase n_s by up to one order of magnitude while noble metals (Rh, Ru, Pd, and Pt) can increase it by up to four orders of magnitude at 950 ℃ as shown in Figure 4-12.

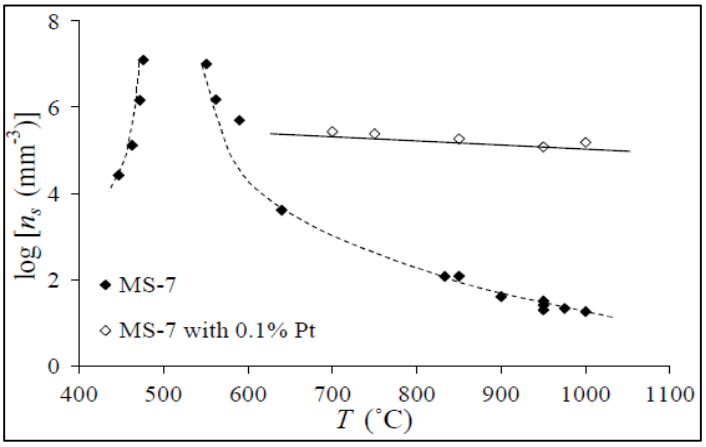

Figure 4-11. The spinel crystal number density (n_s) as a function of temperature for MS-7 and MS-7 with 0.1 % Pt (bulk nucleation). The absence of data between 500 ℃ and 600 ℃ exists because the formed crystals were too small to be detected with optical microscopy.

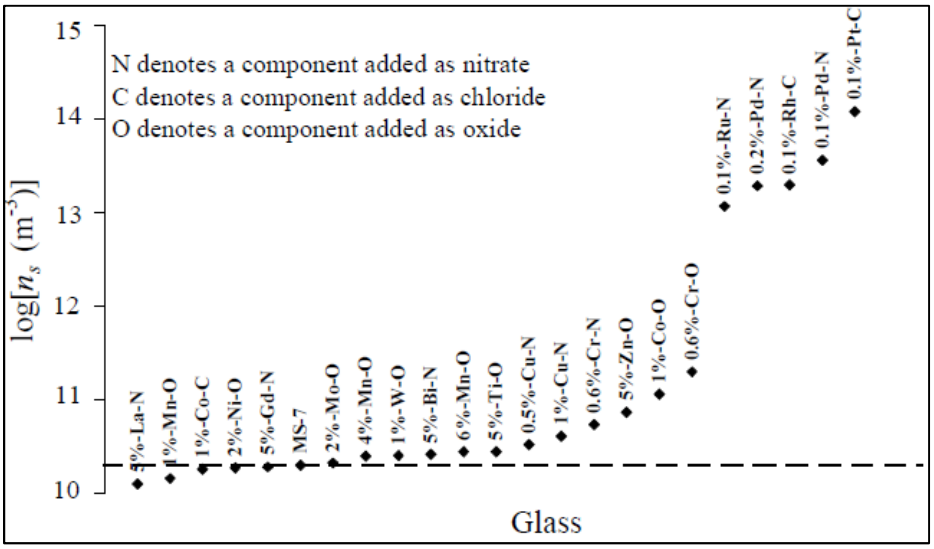

Figure 4-12. The spinel crystal number density (n_s) as a function of components added to MS-7 glass. All glasses were held at 950 ℃ until equilibrium was established.

The idea of increased crystallization in glass due to the presence of nucleation agents is a major problem in HLW vitrification since refractory brick is high in chromium and components in the glass melters are made with Inconel-690 superalloy, which is high in nickel. Thus, gradual erosion and corrosion of the melter will lead to additional Cr and Ni in the glass. Furthermore, melt insoluble particles like ruthenium and rhodium are always present in spent nuclear fuel and defense nuclear waste.

As an aside, the chemistry of ruthenium has been considered in detail in a paper by Schreiber et al.[24] Specifically, the authors showed that extreme conditions, if any, would be necessary to dissolve ruthenium in a borosilicate melt and that the precipitation of RuO_2 from a borosilicate melt appears to be inherent to the system, thus the chemistry of ruthenium in borosilicate melts is dominated by the virtual insolubility of Ru^{IV} as RuO_2. Additionally, extreme oxidizing conditions may produce gaseous RuO_4, whereas extreme reducing conditions may yield metallic ruthenium, nonetheless soluble redox states of ruthenium are not stabilized in the simple borosilicate melt.

Although the chemical conditions in most HLW glasses are clearly very accommodating towards spinel crystallization, there may still be unexplored chemical and/or electromagnetic methods capable of limiting spinel accumulation within HLW melters without requiring changes to the melter design. The next section highlights some research on nepheline crystallization in HLW glass.

5.0 Research Highlights of Nepheline Crystallization in High-Level Waste Glass

One of the significant limitations to higher waste loading in HLW glass is the high concentration of Al_2O_3 and Na_2O found in many waste streams. Aluminum ions are third in total inventory of DOE waste after nitrate and sodium with most of the Al coming from fuel cladding.[52] Consequently, numerous and extensive separation steps have been devised to reduce the Al concentration in waste feed.[53] At the DWPF Al dissolution strategies have been aimed at reducing the mass of Al in order to achieve sludge mass reduction, thereby reducing canister counts and HLW disposal costs. At the WTP, the primary concern with high Al and Na concentration is the formation of nepheline ($NaAlSiO_4$) crystals during canister cooling, as Al will not be removed in pre-vitrification steps. Glass poured in a stainless steel canister is cooled slowly near the canister centerline. This can create a favorable thermal environment for nepheline crystalline phases to form. Since nepheline formation from HLW glass depends largely on the thermal history of a glass, one major obstacle in nepheline crystallization research is that quantitative comparisons of the nepheline mass fraction for glasses formed with different heat treatments may not be relatable, i.e. nepheline formed from a glass during one heat treatment may not form during another heat treatment. This can make it difficult to identify relationships between nepheline formation and glass composition, thereby making it difficult to develop predictive models that sufficiently describe nepheline crystallization.

Unlike spinel crystals which are not detrimental to the chemical durability of the glass, nepheline crystals form by removing important glass-forming constituents from the melt.[52] Consequently, nepheline formation usually results in reduced chemical durability as measured in many different durability tests.[33] Like all crystallization, nepheline formation depends on chemical, thermodynamic, and kinetic factors. Some of the thermodynamic models used to predict nepheline formation were described in detail in Section 3.

Some early work by Li et al.[22b] and Cicero et al.[54], looked at compositional effects on nepheline precipitation and the impact it has on the waste form acceptability.[22b] Li et al. found a simple method for predicting nepheline crystallization in complex (>15 component) waste glass, and stated that the nepheline primary phase field defined by the Na_2O-Al_2O_3-SiO_2 (NAS) ternary system can be used for screening HLW glass prone to nepheline crystallization, although its boundaries for HLW borosilicate glasses are shifted somewhat outside the ternary nepheline field as shown in Figure 5-1. Li et al. also provided some early evidence that showed the presence of nepheline in glass was detrimental for chemical durability using a 7-day PCT[55], which evaluated normalized boron release values. This early work led to the implementation of the nepheline discriminator (Eq. 15) as a process control constraint at the DWPF.[22b] The discriminator relates the concentrations of SiO_2, Na_2O, and Al_2O_3 (as weight fractions in glass) to a critical value of 0.62. If the discriminator ratio falls above 0.62, as is the case in glasses high in SiO_2, then no nepheline should form; however, glasses falling below 0.62 are considered prone to nepheline crystallization, upon slow cooling. This discriminator defines a boundary line on the NAS ternary diagram above which (or toward the SiO_2 corner of the ternary) nepheline is not predicted to crystallize, as shown in Figure 5-2.

$$\frac{SiO_2}{SiO_2+Na_2O+Al_2O_3} > 0.62 \qquad \textbf{(15)}$$

Although the nepheline discriminator imposes a useful restriction on glass compositions in order to avoid unwanted crystallization, it only considers the concentration of species within the NAS ternary despite the complexity of the chemical compositions seen in HLW glass. To this end, several studies were initiated to investigate the effects of B_2O_3 on nepheline formation in borosilicate glasses.[4c, 32] In summary, these studies showed that whereas Al_2O_3 and Na_2O tend to enhance the nepheline crystallization tendency, an increased fraction of B_2O_3 tends to suppress it in some cases.[32]

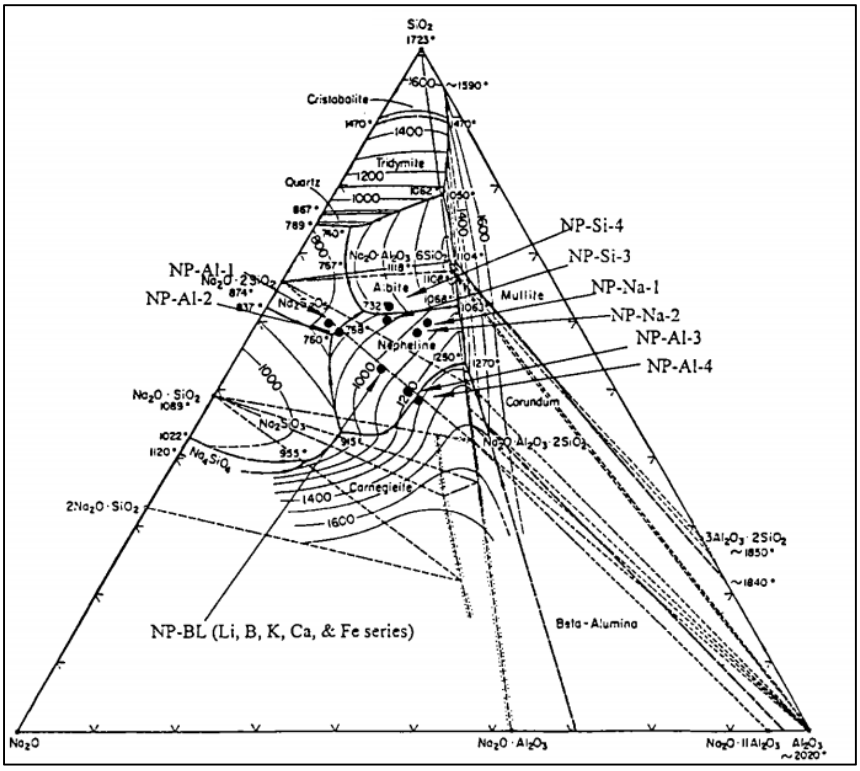

Figure 5-1. Na_2O-Al_2O_3-SiO_2 ternary diagram with various NP waste glasses formulations labeled. Note that most of HLW glasses in Li's study fell into the nepheline-rich phase portion of this diagram.

The suppression of nepheline crystallization in glass by B_2O_3 was further evidenced when Li et al. used Raman spectroscopy to identify nepheline forming quasicrystals as a function of B_2O_3 concentration in complex (> 15 component) waste glass.[4c] A Raman spectroscopy band at 850cm^{-1} was assigned to Al^{IV}-O-Si quasicrystalline units in which tetrahedral Al^{IV} ions are substituted for Si in the glass network, creating $[AlO_{4/2}]^-$ anions that are charge-balanced by Na^+ cations, i.e. $NaAlO_2$. These substituted network units were associated with nanocrystals (aka quasicrystals) that formed in the melts and were preserved in the quenched glass samples The Raman results were confirmed by optical microscopy, scanning electron microscopy, and transmission electron microscopy. These nanocrystals, which resemble nepheline, are described as precursors to nepheline crystals, and the intensity of the Raman band corresponding to these nanocrystalline units was related to the liquidus temperature and the chemical composition of the glass. Specifically, an increase in B_2O_3 and SiO_2 concentrations was found to decrease the Raman band intensity and the liquidus temperature, whereas an increase in Al_2O_3 and Na_2O concentrations increased both. These results suggest that increasing the concentration of Na_2O in high Al_2O_3 containing waste glasses increases the concentration of nepheline forming precursors. Increasing the SiO_2 content decreases the tendency of nepheline formation by diluting the number of available $NaAlO_2$ nepheline forming precursor groups. Increasing the B_2O_3 content of the glass allows the Na_2O to preferentially associate with B_2O_3 thereby leading to the formation of $NaBO_2$ groups which decrease the number of available $NaAlO_2$ nepheline forming groups. Additionally, the effect of increasing B_2O_3 towards inhibiting the formation of nepheline forming groups was stronger than the effect of increasing SiO_2. These findings were similar to the results obtained by X-ray radial distribution function (RDF) analysis on pure nepheline glass[56] and the results of molecular dynamics simulations of glasses in the $NaAlSiO_4$-SiO_2 system.[57]

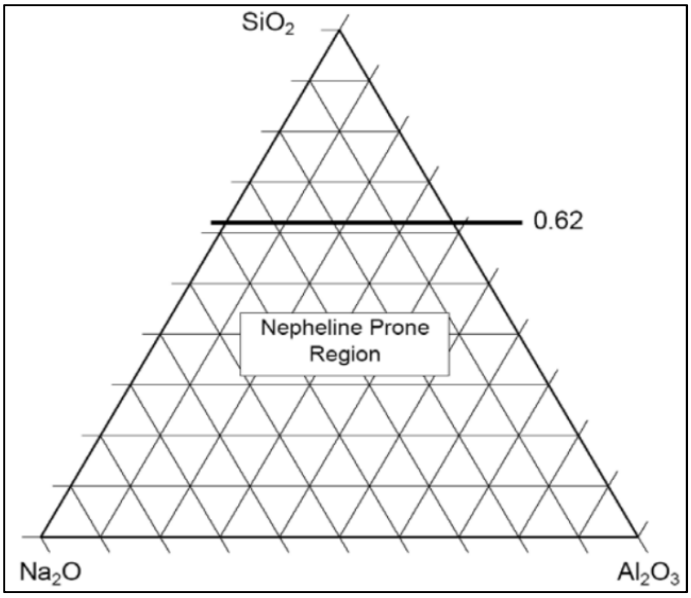

Figure 5-2. Ternary Na_2O- Al_2O_3-SiO_2- diagram showing the location of the current nepheline discriminator. Glasses below the 0.62 line are considered prone to nepheline crystallization.

In an effort to model the effects of B_2O_3 on nepheline formation, thermodynamic simulations utilizing the ChemSage™ software were employed by Besmann et al.[58] The simulations computed the stability region for nepheline in the NAS ternary with 30 wt. % boria and 0 wt. % boria at 800 ℃. The results, displayed in Figure 5-3, show that the simulation model is fairly accurate and predictive when compared with HLW experimental data.

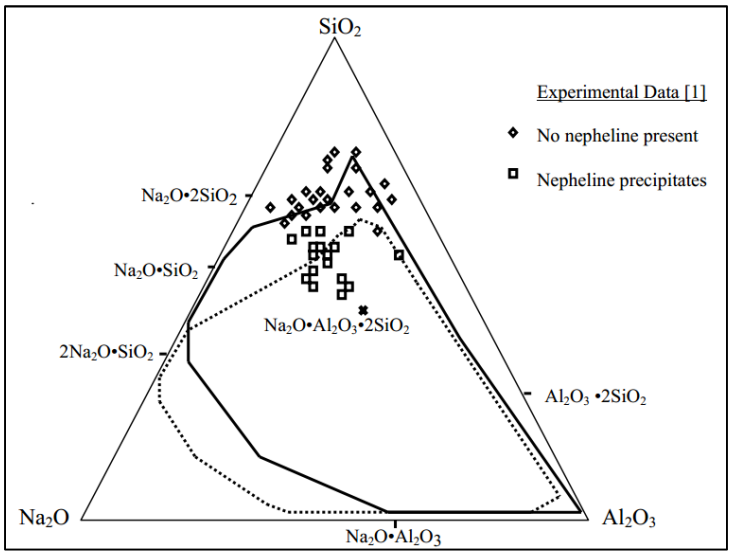

Figure 5-3. NAS Ternary showing the computed stability region for nepheline plus the glass phase at 800 ℃ with no boria (▬) and 30 wt % boria (----) along with experimentally determined data (diamonds and squares).

Following the observations that nepheline formation can sometimes be suppressed by additions of B_2O_3, several studies on a wide range of simplified HLW glasses were conducted to determine whether the nepheline discriminator is an overly conservative process control constraint. As described by Fox et al., "refining the nepheline discriminator to include other important components and to reduce conservatism may provide access to higher waste loadings, decreased washing and improved waste throughput."[59]

In Fox's work, the object was to develop and characterize a series of HLW glass compositions based on a projected composition of Sludge Batch 5 for the DWPF. The selected glass compositions all had nepheline discriminator values below the current limit of 0.62 and covered a range of locations on the Na_2O-Al_2O_3-SiO_2 ternary diagram as shown in Figure 5-4. They also included varying amounts of B_2O_3 and CaO to support an evaluation of the impact of these components on the tendency for nepheline crystallization. Additionally, the glasses were cooled through both rapid quenching on a stainless steel plate and through CCC heat-treatments designed to mimic the thermal conditions along the centerline of a DWPF-canister.

The study showed that nepheline was more prone to form under CCC thermal conditions as opposed to rapid thermal quenching. Specifically, only four out of forty glass compositions formed nepheline or nepheline-like crystals in quenched glass, while fifteen out of forty formed nepheline/nepheline-like crystals upon CCC heat-treatment. In some cases B_2O_3 and increased concentrations of CaO were shown to improve chemical durability responses and suppress the formation of nepheline even though the compositions fell below the nepheline discriminator value. Furthermore, several compositions that targeted higher Al_2O_3 concentrations were shown to be very durable.

Although this work provided some incentive to consider revision of the nepheline discriminator in order to reduce possible conservatism and incorporate the influence of B_2O_3, the overall results were too inconclusive to model.

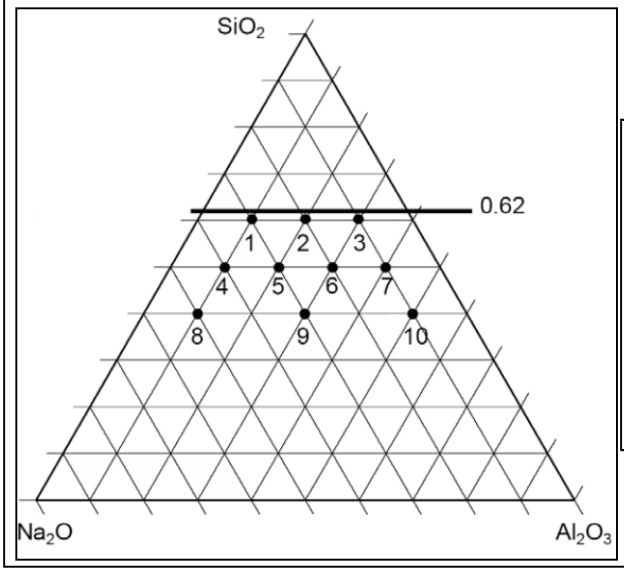

Nepheline Discriminator Value	Na_2O (wt %)	Al_2O_3 (wt %)	SiO_2 (wt %)
0.60	30	10	60
0.60	20	20	60
0.60	10	30	60
0.50	40	10	50
0.50	30	20	50
0.50	20	30	50
0.50	10	40	50
0.40	50	10	40
0.40	30	30	40
0.40	10	50	40

Figure 5-4. (Left): Location of the ten composition points selected on the NAS ternary. (Right): Description of the ten composition points selected on the NAS ternary diagram.

In order to better understand the kinetic properties of nepheline formation, Menkhaus et al. evaluated experimental data on a simplified HLW glass using the KJMA equation similar to the way in which the kinetics of spinel formation was evaluated (see Section 4).[60] The results showed that the nepheline mass fraction as a function of temperature during an isothermal heat-treatment is fairly well described by the KJMA equation. Importantly, the glass composition used in this study, did not contain insoluble noble metals, thus the reliability of the reported results with respect to understanding nepheline in HLW glass is somewhat questionable. Additionally, the glass composition was found to lie near the eutectic point in Figure Figure 4-4 The kinetic parameters extracted from the KJMA analysis for nepheline are compared with those obtained from spinel and clinopyroxene in Table 5-1. The kinetic results can be summarized as follows: The concentrations of nepheline and clinopyroxene can be more than ten times higher than spinel as indicated by the large C_{max} values obtained from the KJMA fit, although this only occurs when nepheline is formed from the melt on the nepheline side of the binary, not if it is formed in the nepheline subsolidus region.

Table 5-1. Kinetic and Equilibrium Coefficients for Nepheline, Spinel, and Clinopyroxene Crystallization in High-Level Waste Glasses

Phase	T_L (K)	C_{max}	B_L (K)	n	$B\tau$ (K)	τ_0 (s)
Nepheline	1193	0.6317	3972	1.5	24360	1.41×10^{-9}
Spinel	1337	0.0371	3783	1.5	14250	6.31×10^{-3}
Clinopyroxene	1004	0.2030	44302	2.5	5849	4.92×10^{-3}

The B_L values for nepheline and spinel are similar and low, thus indicating that the equilibrium concentration of these phases increases gradually as temperature decreases. The B_τ value indicates how rapidly the rate of crystal growth increases as temperature decreases. According to the B_τ values nepheline crystal growth appears more sensitive to temperature change than spinel or clinopyroxene. The most striking aspect of this kinetic data is the τ_0 values, which give some indication of the rate at which various crystalline phases can form from a melt. The τ_0 value for nepheline is nearly six orders of magnitude smaller than it is for spinel or clinopyroxene, thus nepheline crystallization appears to be very rapid. The KJMA equation showed that at certain temperatures the time to bring nepheline concentration close to equilibrium can be as short as 1 minute.

6.0 Conclusions and Path Forward

The possibility of generating solid crystals, both before and after HLW glass has been poured, presents some serious concerns and poses many questions for researchers. With this in mind, the following list provides several suggestions for research that might contribute to glass processing improvement.

It is suggested that experiments be designed to investigate the following questions:

- If solid spinel crystals were to accumulate inside of a melter or spinel and/or acmite[61] were to accumulate in the glass discharge riser, at what concentration would these crystals become severely problematic for the melter?
- If spinel crystallization were allowed to occur inside a melter, as has been proposed for WTP melters, is there an in-situ way to detect the accumulation of these solids? Conversely, are pilot-scale tests, as were previously performed for the DWPF melter, the only way to develop an understanding of how crystal accumulation will occur when operating under a waste loading environment that prompts spinel crystallization?
- Can the glass process (pouring rates, waste pre-treatment, riser design, etc.) be improved or modified to prevent or limit crystal accumulation inside a melter under higher waste loadings?
- What volume of glass in a canister experiences the time and temperature conditions that drive nepheline formation?
- Are data generated from different cooling cycles (DWPF vs. WTP) impacting the ability to develop models to resolve nepheline crystallization issues?
- How are the kinetics of spinel and nepheline crystallization effected by the presence of noble metals?
- How is nepheline formation in a waste canister affected by the presence of noble metals?
- Since HLW will always have insoluble particles in the melt, how can glass processing be improved to limit the time that the glass spends in the growth region of nepheline crystallization?

Amoroso has shown that computer simulations of the thermal conditions within a DWPF canister during HLW glass pouring may be useful as a guide for lab-scale research seeking to understand the thermal conditions for nepheline crystallization, although experiments that utilize the simulated thermal data, have yet to be performed.[62] To this end, thermal models, which mimic the conditions inside of a WTP canister, should be developed and laboratory experiments designed, in order to determine how/whether nepheline crystallizes from HLW glass under the currently proposed WTP glass pouring processes.

Future experiments might also consider exploring whether heterogeneous crystallization can be limited by melting and cooling glass inside of vessels or on metal coupons with varying surface compositions/textures. Examining whether different surfaces can affect crystallization may be a worthwhile undertaking. In fact, a report by Amoroso in 2011 showed that certain glass compositions appear to nucleate nepheline at glass interfaces, but not in the bulk.[63]. This result suggests that some glass compositions may preferentially nucleate at the surface of a melting vessel, which, importantly, will not be present as glass cools at the center of a waste canister. Therefore, while this type of nucleation may occur on a laboratory scale, it may not occur in an actual waste canister, where glass cools mostly in the absence of the canister surface.

In terms of limiting nepheline formation, it may be worthwhile to design new ways to rapidly cool HLW melts once they are poured. One such way to increase glass cooling rates may be to place waste canisters on a rotating platform. By rotating the waste canister and generating centrifugal force, it should be possible to force glass towards the cool walls of a canister, thus speeding up the rate at which it cools.

It also appears fruitful to use TTT diagram to extract kinetic information of waste glasses, as was done for DWPF-related glasses in 1984 by Bickford and Jantzen[17]. Currently, a wealth of TTT data exists for DWPF waste glasses.[54 64] However, additional kinetic analyses have not been performed using these TTT diagrams. Thus, it is recommended that such kinetic analysis be performed.

The observation by Li et al.[4c] that B_2O_3 can associate with Na^+ to limit the number of available $NaAlO_2$ nepheline forming groups might be useful for developing experiments which study the effects of other ions on nepheline crystallization. If B_2O_3 and CaO can sometimes restrict nepheline formation, even in glasses that fail the nepheline discriminator test, are there other chemical additives that can also limit its formation? One can devise multifarious experiments to determine the role of chemical additives towards restricting nepheline crystallization. It may be worthwhile to determine whether other 3+ ions or group III metals (like Ga^{3+}, In^{3+}) can also associate with Na^+ in order to limit its availability for nepheline, although Ga^{3+} and In^{3+} are very expensive and their use may be cost prohibitive. Additionally, one must consider that approximately 7 wt. % of nepheline was found to contain Fe^{3+}, thus not all 3+ ions are able to limit Na availability and the formation of nepheline.[36] A more cost effective alternative might be to study the role of a flux (like GeO_2) on nepheline formation. Or to study the combined effects of Li^+ and B^{3+} instead of B^{3+} and Ca^{2+}, because there is no Li nepheline analogue. Phosphorous may be another species worth investigating, but in small amounts as DWPF has a P_2O_5 limit for phase separation. It may also be helpful to revisit existing data, regarding the role of B_2O_3 and CaO on nepheline formation, with more scrutiny.

The inherent caveat with a chemical additive approach towards limiting crystallization is that it requires the addition of more glass forming chemicals into the melt, a process which might contribute negatively to the overall cost of running the HLW vitrification process, depending on how much improvement (higher waste loading) could be made to the vitrification process. A balance would have to be drawn between the benefits of avoiding nepheline crystallization and the drawbacks of adding chemical components to a nepheline forming waste glass

One method that has yet to be explored in limiting crystal accumulation is the use of electromagnetic radiation to selectively heat solid particles (within the melt) above their melting temperature. This type of heating would be useful in the low temperature regions within the HLW melter where crystals are prone to form and/or accumulate, and where Joule heating is limited. Exploiting the quantum mechanical nature of solid crystals rather than the chemical nature might be a convenient route towards limiting crystal accumulation in a HLW melter under dynamic chemical and thermal conditions. Also, the dissolution of crystals via heat would not require the addition of chemical additives and thus would not contribute to producing greater volumes of glass and would not introduce the potential of changing waste form compliant glass to non-waste form compliant glass. In addition to the selective, fast, and low energy heating of molecules via the dielectric effect, the viability of incorporating a microwave system into a HLW melter might be high, due to the simplicity and workability of the electronic components, although the high radiation environment would likely require that modifications be made to the microwave system (e.g. isolation or shielding of sensitive electronic components). The feasibility of microwave induced dissolution of crystals seems high and numerous observations have been reported in the literature, which show improved mass transport and solid-state reaction rates during microwave heating or processing of a variety of ceramic, glass, and polymer materials.[65] The use of microwave selective heating has been recently applied to spinel nanoparticles in a study where the particles were used as catalysts for the formation of formaldehyde.[66] It is acknowledged that none of the aforementioned studies were performed in a radiation field, which would be ubiquitous in a HLW melter.

There is indeed a fundamental need to continue research aimed at comprehensively understanding nepheline and spinel formation in HLW glass; however, the complexity of HLW glass and the intricate interplay between compositional and kinetic factors does not make the path forward an easy one. Nonetheless, fundamental experiments seeking to elucidate these mechanisms may go a long way towards

improving waste loading and waste throughput. While much has been done in recent years to understand how thermal factors affect crystallization, there is much room left to expand our knowledge on the kinetic and compositional drivers of crystallization in HLW glass. Therefore, research in this area must continue if we are to develop new methods to improve the waste vitrification process.

7.0 References

1. Varshneya, A. K., *Fundamentals of Inorganic Glasses*. Harcourt Brace & Company: 1994.
2. (a) Rawlings, R. D.; Wu, J. P.; Boccaccini, A. R., Glass-ceramics: Their production from wastes—A Review. *J Mater Sci* **2006,** *41* (3), 733-761; (b) Stookey, S. D., Catalyzed Crystallization of Glass in Theory and Practice. *Industrial and Engineering Chemistry* **1959,** *51* (7), 805-808.
3. Zakery, A.; Elliott, S. R., Optical properties and applications of chalcogenide glasses: a review. *Journal of Non-Crystalline Solids* **2003,** *330* (1–3), 1-12.
4. (a) H., L.; Vienna, J. D.; Hrma, P.; Smith, D. E.; Schweiger, M. J., Nepheline Precipitation in High-Level Waste Glasses: Compositional Effects and Impact on the Waste Form Acceptability. *Proceedings of MRS* **1997,** *465* (Scientific Basis for Nuclear Waste Management); (b) Hrma, P.; Vienna, J.; Crum, J.; G., P., Liquidus Temperature of High-Level Waste Borosilicate Glasses with Spinel Primary Phase. *Mat. Res. Soc. Symp. Proc.* **2000,** *608*, 671-675; (c) Li, H.; Hrma, P.; Vienna, J. D.; Qian, M.; Su, Y.; Smith, D. E., Effects of Al_2O_3, B_2O_3, Na_2O, and SiO_2 on Nepheline Formation in Borosilicate Glasses: Chemical and Physical Correlations. *J. Non-Cryst. Solids* **2003,** *331*, 202-216; (d) R.P. Turcotte, J. W. W., R.P. May, *Scientific Basis for Nuclear Waste Management*. Materials Research Society: 1980; Vol. 2.
5. Brown Jr, G. E.; Farges, F.; Calas, G., *X-Ray Scattering and X-Ray Spectroscopy Studies of Silicate Melts*. Mineralogic Society of America: Washington, DC, 1995; Vol. 32.
6. Burnham, W., The Nature of Multicomponent Aluminosilicate Melts. *Phys. Chem. Earth* **1981,** *13 and 14*, 191-227.
7. Jantzen, C. M.; Krepski, R. P.; Herman, H., Ultra-rapid Quenching of Laser-Melted Binary and Unary Oxides. *Mat. Res. Bull.* **1980,** *15* (9), 1313-1326.
8. Schuller, S.; Pinet, O.; Grandjean, A.; Blisson, T., Phase separation and crystallization of borosilicate glass enriched in MoO3, P2O5, ZrO2, CaO. *Journal of Non-Crystalline Solids* **2008,** *354* (2–9), 296-300.
9. Thompson, D. P., Materials science: Cooking up tougher ceramics. *Nature* **2002,** *417* (6886), 237-237.
10. Hamzawy, E. M. A.; El-Meliegy, E. A. M., Preparation of Nepheline Glass-Ceramics for Dental Applications. *Materials Chemistry and Physics* **2008,** *112*, 432-435.
11. Wood, R., Future hard disk drive systems. *Journal of Magnetism and Magnetic Materials* **2009,** *321* (6), 555-561.
12. Jantzen, C. M.; Bickford, D. F., Leaching of Devitrified Glass Containing Simulated SRP Nuclear Waste. *Sci. Basis for Nuclear Waste Management VIII* **1985,** *C. M. Janzten, J. A. Stone, and R. C. Ewing* (Materials Research Society, Pittsburgh, PA 135-146).
13. Matyas, J.; Huckleberry, A. R.; Rodriguez, C. P.; Lang, J. B.; Owen, A. T.; Kruger, A. A. Crystal-Tolerant Glass Approach For Mitigation of Crystal Accumulation in Continuous Melters Processing Radioactive Waste. http://www.hanford.gov/files.cfm/crystal-tolerant-glass-approach.pdf.
14. (a) Jantzen, C. M.; Brown, K. G., Predicting the spinel-nepheline liquidus for application to nuclear waste glass processing. Part I: Primary phase analysis, liquidus measurment, and quasicrystalline approach. *J. Am. Ceram. Soc.* **2007,** *90* (6), 1866-1879; (b) Jantzen, C. M.; Brown, K. G., Predicting the spinel-nepheline liquidus for application to nuclear waste glass processing. Part II: Quasicrystalline freezing point depression model. *J. Am. Ceram. Soc.* **2007,** *90* (6), 1880-1891.
15. Best, B. Physical Parameters of Cooling in Cryonics. http://www.benbest.com/cryonics/cooling.html.
16. Shelby, J. E., *Introduction to Glass Science and Technology*. The Royal Society of Chemistry: 1997.
17. Jantzen, C. M.; Bickford, D. F.; Karraker, D. G.; Wicks, G. G., Time-Temperature-Transformation Kinetics in SRL Waste Glass. *Advances in Ceramics, 8, American Ceramic Society, Westerville, OH, 30-38* **1984**.

18. Bickford, D. F.; Jantzen, C. M., Devitrification of SRL Defense Waste Glass. *Sci. Basis for Nuclear Waste Management VII, G.L McVay (ed). Elsevier Publ., New York* **1984**, 557-565.
19. Bickford, D. F.; C.M, J., Devitrification of Defense Nuclear Waste Glasses: Role of Melt Insoluble. *J. Non-Cryst. Solids* **1986,** *84* (1-3), 299-307.
20. Reynolds, J. G.; Hrma, P., *Scientific Basis for Nuclear Waste Management XX*. Materials Research Society: Warrendale, PA, USA, 1997; Vol. 465.
21. Hrma, P., Crystallization during processing of nuclear waste glass. *Journal of Non-Crystalline Solids* **2010,** *356* (52–54), 3019-3025.
22. (a) Goel, A.; McCloy, J. S.; Fox, K. M.; Leslie, C. J.; Riley, B. J.; Rodriguez, C. P.; Schweiger, M. J., Structural analysis of some sodium and alumina rich high-level nuclear waste glasses. *Journal of Non-Crystalline Solids* **2012,** *358* (3), 674-679; (b) Li, H.; Vienna, J. D.; Hrma, P.; Smith, D. E.; Schweiger, M. J., Nepheline Precipitation in High-Level Waste Glasses: Compositional Effects and Impact on the Waste Form Acceptability. *Proceedings of MRS* **1997,** *465* (Scientific Basis for Nuclear Waste Management).
23. Doremus, R. H., *Glass Science*. 2 ed.; John Wiley & Sons, Inc.: 605 Third Avenue, New York, NY, 1994.
24. Schreiber, H. D.; Settle Jr, F. A.; Jamison, P. L.; Eckenrode, J. P.; Headley, G. W., Ruthenium in glass-forming borosilicate melts. *Journal of the Less Common Metals* **1986,** *115* (1), 145-154.
25. Muan, A., Stability Relations Among Some Manganese Minerals. *The American Mineralogist* **1959,** *44* (September-October).
26. Bragg, L.; Claringbull, G. F., *Crystal Structure of Minerals In the Crystalline State*. G. Bell and Sons Ltd: London, 1965; Vol. IV.
27. Landon, L. F., Preliminary Technical Data Summary No. 3 for the Defense Waste Processing Facility. *DPSTD-77-13-3* **1980**.
28. Matyas, J.; Klouzek, J.; Nemac, L.; Trochta, M., *"Spinel Settling in HLW Melters", In Proceedings of the 8th International Conference on Radioactive Waste Management and Environmental Remediation: ICEM'01: held in Bruges, Belgium, September 30-October 4, 2001, 3, Edited by A. Taboas, R. Vanbrabant, and G. Benda. The American Society of Mechanical Engineers, New York, NY.* . p 1787-1792.
29. (a) Jantzen, C. M.; Imrich, K. J.; Brown, K. G.; Pickett, J. B., High Chrome Refractory Characterization: Part I. Impact of Melt Reduction/Oxidation (REDOX) on the Corrosion Mechanism in Radioactive Waste Glass Melters. *Int. J. Appl. Glass Sci* **2015**; (b) Jantzen, C. M.; Imrich, K. J.; Brown, K. G.; Pickett, J. B., High Chrome Refractory Characterization: Part II. Accumulation of Spinel Corrosion Deposits in Radioactive Waste Glass Melters. *Int. J. Appl. Glass Sci* **2015**.
30. Jantzen, C. M.; Cozzie, A. D.; Bibler, N. E., High Level Waste (HLW) Processing Experience with Increased Waste Loadings (U). *WSRC-MS-2004-00286, Rev. 0* **2004**.
31. Jantzen, C. M.; Cozzie, A. D.; Bibler, N. E., Characterization of Defense Waste Processing Facility (DWPF) Glass and Deposit Samples from Melter #2 (U). *WSRC-TR-2003-00504, Rev. 0* **2003**.
32. (a) Li, H.; Jones, B.; Hrma, P.; Vienna, J. D., *Ceram. Trans.* **1998**, 279; (b) Li, H.; Vienna, J. D.; Hrma, P.; Smith, D. E.; Schweiger, M. J., *Mater. Res. Soc. Proc.* **1997,** *465*, 261.
33. Jantzen, C. M.; Bickford, D. F., Leaching of Devitrified Glass Containing Simulated SRP Nuclear Waste. *Sci. Basis for Nuclear Waste Management VIII, C.M. Jantzen, J. A. Stone, R. C. Ewing (eds), Materials Research Society, Pittsburgh, PA 135-146* **1985**.
34. Rushton, M. J. D.; Grimes, R. W.; Owens, S. L., Changes to Alkali Ion Content Adjacent to Crystal-Glass Interfaces. *Sci. Basis for Nuclear Waste Management XXXI, W. E. Lee, J. W. Roberts, N. C. Hyatt, R. W. Grimes (eds), Materials Research Society, Pittsburgh, PA, 207-213* **2008**.
35. Tovena, I.; Advocat, T.; Ghaleb, D.; Vernaz, E.; Larche, F., Thermodynamic and Structural Models Compared with the Initial Dissolution Rate of SON Glass Samples. *Sci. Basis for Nuclear Waste Management XVII, A. Barkatt and R. A. VanKonynenburg (eds), Materials Research Society, Pittsburgh, PA, 595-602* **1994**.

36. Jantzen, C. M.; Brown, K. G., Impact of Phase Separation on Waste Glass Durability. *Environmental Issues and Waste Management Technologies in the Ceramic and Nuclear Industries, V. G. T. Chandler (Ed.), Ceramic Transactions, V. 107, 289-300* **2000**.
37. I., O. M.; Lee, W. E., Topologically Disordered Systems at the Glass Transition. *J. Phys. Condens. Matter* **2006,** *18*, 11507-11520.
38. Peeler, D. K., Batch 1 Variability Study Using Twice Washed Tank 51 Sludge. *WSRC-RP-1045, Rev. 1* **1995**.
39. Peeler, D. K., Batch 1 Variability Study Using Twice Washed Tank 51 Sludge and Frit 200. *WSRC-RP-96-20, Rev. 0* **1996**.
40. Harbour, J. R.; Edwards, T. B.; Workman, R. J., Summary of Results for Macrobatch 3 Variability Study. *WSRC-TR-2000-00351, Rev. 0* **2000**.
41. Herman, C. C.; Edwards, T. B.; Marsh, D. M., Summary of Results for Expanded Macrobatch 3 Variability Study. *WSRC-TR-2001-00511, Rev. 0* **2001**.
42. Jantzen, C. M.; Brown, K. G.; Pickett, J. B., Durable Glass for Thousands of Years. *Int. J. Appl. Glass Sci* **2010,** *1*, 38-62.
43. Bickford, D. F.; Jantzen, C. M., *Devitrification of SRL Defense Waste Glass*. Elsevier, New York: Scientific Basis for Nuclear Waste Management VII, 1984; p 557-565.
44. Edwards, T. B.; G., B. K.; Postles, R. L., *"SME Acceptability Determination for DWPF Process Control", U.S. Department of Energy Report WSRC-TR-95-00364, Revision 5, Washington Savannah River Company, Aiken, SC, (2006)*.
45. Williams, R. J. P., Deposition of Trace Elements in Basic Magmas. *Nature* **1959,** *184*, 144.
46. Roeder, P. L., Activity of Iron and Olivine Solubility in Basaltc Liquids. *Earth Planetary Sci. Lett.* **1974,** *23*, 397-410.
47. Brown, K. G.; Jantzen, C. M.; Ritzhaupt, G., Relating Liquidus Temperature to Composition for Defense Waste Processing Facility (DWPF) Process Control (U). *U.S. Department of Energy Report WSRC-TR-2001-00520, Rev. 0, Westinghouse Savannah River Company, Aiken, SC (2001)*.
48. Levin, I. N., *Physical Chemistry*. 2nd ed.; McGraw-Hill Book Company: New York, NY, 1983.
49. Mika, M.; M.J., S.; Hrma, P., *Liquidus Temperature of Spinel Precipitating High-Level Waste Glass*. 1997; Vol. 465.
50. (a) Turcotte, R. P.; Wald, J. W.; May, R. P., *Scientific Basis for Nuclear Waste Management*. Materials Research Society: Warrendale, PA, USA, 1980; Vol. 2; (b) Marra, S. L.; Andrews, M. K.; Cicero, C. A., *Environmental and Waste Management Issues in The Ceramic Industry*. American Ceramic Society: Westerville, OH, 1993; Vol. 39; (c) Klouzek, J.; Alton, J.; Hrma, P.; Plaisted, T. J., *Ceramic Transactions*. American Ceramic Society: Westerville, OH, 2001; Vol. 119; (d) Plaisted, T. J.; Alton, J.; Wilson, B.; Hrma, P., *Ceramic Transactions*. American Ceramic Society: Westerville, OH, USA, 2001; (e) Alton, J.; Plaisted, T. J.; Hrma, P., Dissolution and growth of spinel crystals in a borosilicate glass. *Journal of Non-Crystalline Solids* **2002,** *311* (1), 24-35.
51. Alton, J.; J. Plaisted, T.; Hrma, P., Kinetics of growth of spinel crystals in a borosilicate glass. *Chemical Engineering Science* **2002,** *57* (13), 2503-2509.
52. McCloy, J. S.; Schweiger, M. J.; Rodriguez, C. P.; Vienna, J. D., Nepheline Crystallization in Nuclear Waste Glasses Progress Toward Acceptance of High-Alumina Formulations. *Int. J. Appl. Glass Sci* **2011,** *2*, 201-214.
53. (a) Certa, P. J.; Well, M. N., River Protection Project System Plan. *Office of River Protection* **2010,** *Revision 5* (ORP-11242); (b) Vienna, J. D., Nuclear Waste Vitrification in the United States: Recent Developments and Future Options. *Int. J. Appl. Glass Sci* **2010,** *1* (3), 309-321.
54. Cicero, C. A.; Marra, S. L.; Andrews, M. K., Phase Stability Determinations of DWPF Waste Glasses (U). *WSRC-TR-93-227, Rev. 0* **1993**.
55. C1285-14, A., Standard Test Methods for Determining Chemical Durability of Nuclear, Hazardous, and Mixed Waste Glasses and Multiphase Glass Ceramics: The Product Consistency Test (PCT). *Books of Standards Volume: 12.01*.

56. Taylor, M.; Brown, G. E., Structure of Mineral Glasses-II. The SiO_2-$NaAlSiO_4$ Join. *Geochim. Cosmochim. Acta* **1979,** *43*, 1467-1479.
57. Stein, D. J.; Spera, F. J., Molecular Dynamics Simulations of Liquids and Glasses in the System $NaAlSiO_4$-SiO_2: Methodology and Melt Structures. *Am. Miner.* **1995,** *80*, 417-431.
58. Besmann, T. M.; Spear, K. E., Thermochemical Modeling of Oxide Glasses. *J. Am. Ceram. Soc.* **2002,** *85*, 2887-2894.
59. (a) Fox, K. M.; Edwards, T. B., Refinement of the Nepheline Discriminator: Results of a Phase I Study. *SRNS-STI-2008-00099, Rev. 0*; (b) Fox, K. M.; Edwards, T. B., Refinement of the Nepheline Discriminator: Results of a Phase II Study. **2008,** *SRNS-STI-2008-00099, Rev. 0*.
60. Menkhaus, T. J.; Hrma, P.; Li, H., Kinetics of Nepheline Crystallization From High-Level Waste Glass. In *Ceramic Transactions*, Chandler, G. T.; Feng, X., Eds. Ceramic Transactions: Westerville, OH, 1999; Vol. 107.
61. Jantzen, C. M., Devitrification of Scale Melter Glass in Riser Heater. *U. S. DOE Report DPST-86-461* **1986**.
62. Amoroso, J., Computer Modeling of High-Level Waste Glass Temperatures Within DWPF Canisters During Pouring and Cool Down. *U.S. Department of Energy Report SRNL-STI-2011-00546, Rev. 0, Savannah River National Laboratory, Aiken, SC (2011)*.
63. Amoroso, J. W., The Impact of Kinetics on Nepheline Formation in Nuclear Waste Glasses. *SRNL-STI-2011-00051, Rev. 0* **2011**.
64. Billings, A. L.; Edwards, T. B., Time-Temperature Transformation (TTT) Diagrams for Future Waste Compositions. *SRNL-STI-2010-00373, Rev. 0* **2010**.
65. (a) Almeida, F. J. M.; Martinelli, J. R.; Partiti, C. S. M., Characterization of iron phosphate glasses prepared by microwave heating. *Journal of Non-Crystalline Solids* **2007,** *353* (52-54), 4783-4791; (b) Ghussn, L.; Martinelli, J. R., A novel method to produce niobium phosphate glasses by microwave heating. *J Mater Sci* **2004,** *39* (4), 1371-1376; (c) Mahmoud, M. M.; Folz, D. C.; Suchicital, C. T. A.; Clark, D. E., Crystallization of Lithium Disilicate Glass Using Microwave Processing. *J. Am. Ceram. Soc.* **2012,** *95* (2), 579-585; (d) Mandal, A. K.; Balaji, S.; Sen, R., Microwave and conventional preparation of Zinc borate glass: Eu3+ ion as luminescent probe. *Journal of Alloys and Compounds* **2014,** *615* (0), 283-289; (e) Tian, Y.; Zuo, W.; Chen, D., Crystallization evolution, microstructure and properties of sewage sludge-based glass–ceramics prepared by microwave heating. *Journal of Hazardous Materials* **2011,** *196* (0), 370-379; (f) Vaidhyanathan, B.; Ganguli, M.; Rao, K. J., A Novel Method of Preparation of Inorganic Glasses by Microwave Irradiation. *J. Solid State Chem.* **1994,** *113* (2), 448-450; (g) Zhao, W.; Chen, J.; Chang, X.; Guo, S.; Srinivasakannan, C.; Chen, G.; Peng, J., Effect of microwave irradiation on selective heating behavior and magnetic separation characteristics of Panzhihua ilmenite. *Applied Surface Science* **2014,** *300* (0), 171-177.
66. Crosswhite, M.; Hunt, J.; Southworth, T.; Serniak, K.; Ferrari, A.; Stiegman, A. E., Development of Magnetic Nanoparticles as Microwave-Specific Catalysts for the Rapid, Low-Temperature Synthesis of Formalin Solutions. *ACS Catalysis* **2013,** *3* (6), 1318-1323.
67. Reed-Hill, R. E.; Abbaschian, R., *Physical Metallurgy Principles*. 3 ed.; PWS Publishing Company: Boston, MA, 1994.
68. Gordon, P., *Principles of Phase Diagrams in Materials Systems*. McGraw-Hill Book Company: 1968.

8.0 Appendix

This section describes the basics of homogeneous nucleation.

Although nucleation and growth are both a part of crystallization, they typically occur within different temperature ranges as shown in Figure 8-1. Since growth cannot precede nucleation, and since each process tends to happen within different temperature ranges, it should become obvious that the thermal history of a material plays an important role in determining whether or not homogeneous crystallization can occur. For example, consider a pure glass system (one in which there are no insoluble particles, bubbles, etc.) that is heated above its liquidus temperature (T_L), i.e. the temperature at which a crystal and a liquid can exist in equilibrium. If this system is allowed to cool from $T > T_L$ (where in principle it should be purely liquid) it will not possess nucleation sites as the temperature cools through the growth region. Thus, this system can only undergo crystallization within the temperature region where both nucleation and growth overlap.

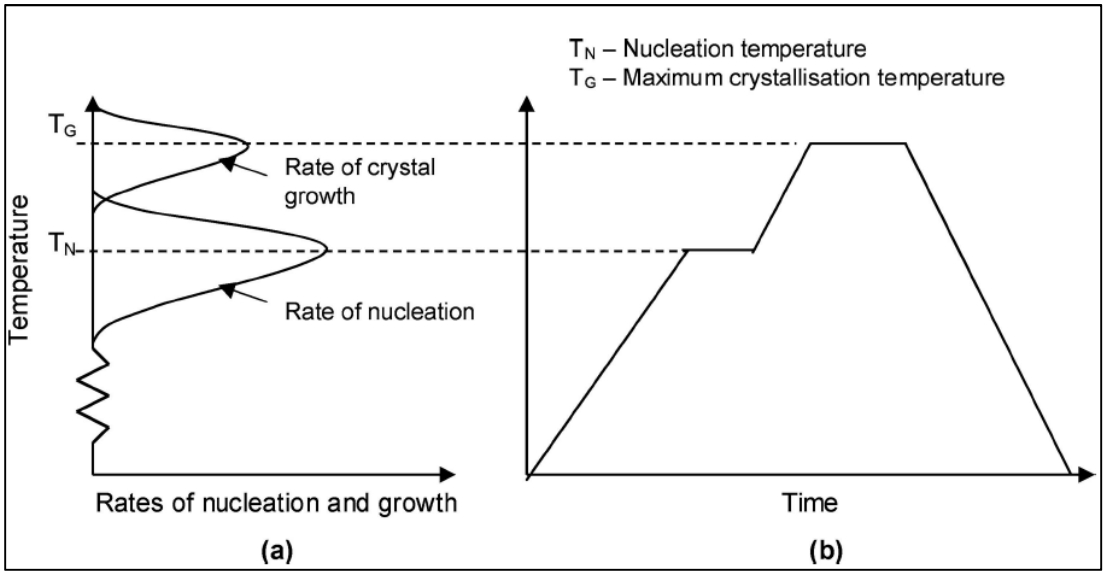

Figure 8-1. (a) Temperature dependence of the nucleation and growth rates in a system with very small overlap between the rate curves. (b) A time-temperature diagram of a two-stage heat treatment for producing crystalline glass when a small overlap exists between the nucleation and growth temperature regions.

In Figure 8-1 this is a narrow temperature range concurrent with low rates of nucleation and growth. As a result, crystallization in this system would be negligible. Additionally, since no nucleation sites were present in this system within a temperature range well below T_L, the system is said to have reached the metastable, supercooled liquid state.

If however, the same glass system is heat treated in such a way that it is allowed to slowly pass through the temperature region where nucleation is favored, followed by heating through the region where growth is favored, and the sample is cooled before reaching $T > T_L$, then an appreciable amount of crystals should be found in the glass. The amount and size of these crystals are dependent on the amount of time the system spends in the nucleation and growth regions. For example, if the system was allowed to dwell within the temperature region where the rate of nucleation is large, then in principle it should form a large number of nucleation sites, which can then be grown into a large number of small crystals. The large

number of crystals is consistent with the formation of a large number of nucleation sites that formed during the heat treatment. If the same system undergoes a heat-treatment where it passes through the nucleation stage quickly, but is allowed ample time to dwell in the growth region, the sample should contain large, but less-abundant crystals. Additionally, if impurities like insoluble particles are placed in this glass system, one would expect to find crystal formation, regardless of the heat-treatment, provided that the system spends some time in the growth temperature region. This is because the melt-insoluble particles act as nucleation sites. The ability to use thermal history and implanted nucleation sites to control crystal quantity and size in a glass is of fundamental important in glass technology.

It is worth noting that a good glass-forming system is one in which the overlap between growth and nucleation is small, thus the propensity for crystallization is low when cooling from the melt; however, the overlap of nucleation and growth temperature regions is compositionally dependent and can be somewhat tailored to generate a specific type of material. Figure 8-2 shows the temperature dependence of the nucleation and growth rates in a system with a significant overlap. This type of system would be more prone to crystallization since crystal formation can be achieved using a single-stage cooling or heating treatment as shown in Figure 8-2(b).

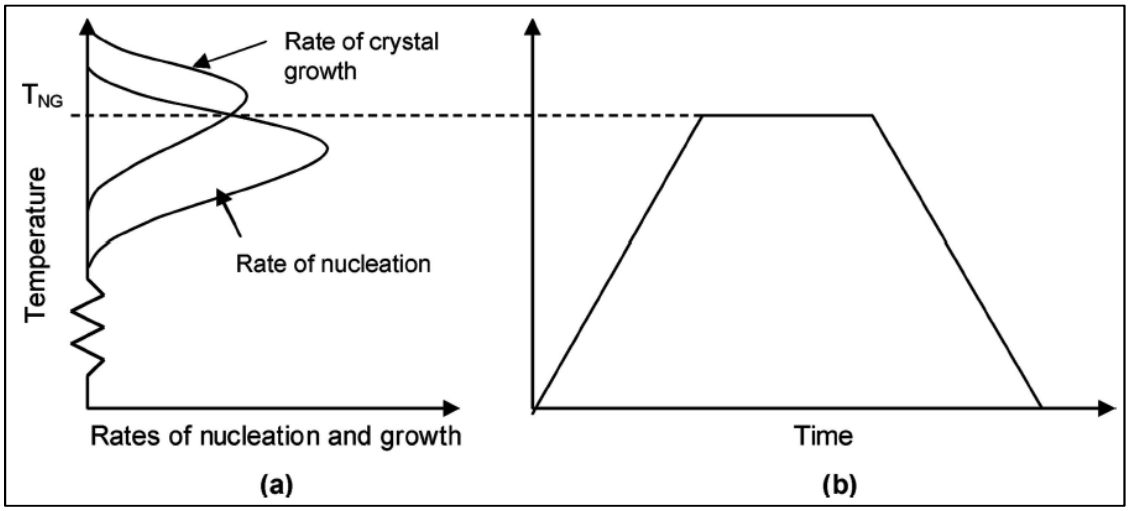

Figure 8-2. (a) Temperature dependence of the nucleation and growth rates with a large overlap between the rate curves. (b) A time-temperature diagram of a single-stage heat treatment for producing highly crystalline glass when a large overlap exists between the nucleation and growth temperature regions.

Clearly, the thermal history and overlap of the nucleation and growth temperature regions is of great importance when considering the tailored or unwanted crystallization of glass. The thermal history is also important in making accurate measurements of a glass' true liquidus temperature, which is a vital parameter in optimizing glass processing conditions. A measured liquidus temperature, obtained from a 'high-to-low temperature heat-treatment', can be lower than the true liquidus temperature, since the liquid can enter the metastable supercooling zone below T_L without appreciable crystallization occurring, due to the lack of nucleation sites. Consequently, accurate liquidus temperatures, like those measured at SRNL and PPNL, are usually obtained by a 'low-to-high heat-treatment' since nuclei formed at low temperatures will be present as the system reaches the growth temperature, thus crystals will begin to form at the precise liquidus temperature[67]; however, this is not always the case. In HLW glass where insoluble nucleation sites are ever-present, the same T_L can be obtained regardless of whether the measurement was performed by a high-to-low or low-to-high treatment.[19] It is worth noting that liquidus measurements near a eutectic point can be more complex, i.e. more susceptible to impact from

undercooling rate and/or direction, than in other regions in a phase diagram.[68] In the processing of HLW at the DWPF, the liquidus temperature is required to be at least 100 ℃ below the nominal melter operating temperature. This process control limit is designed to prevent unwanted bulk crystallization within the melt pool, but it can restrict access to higher waste loadings. It is therefore vital to know the liquidus temperature of a glass composition used for immobilization of HLW.

Distribution:

J. W. Amoroso, 999-W
T. B. Brown, 773-A
A. S. Choi, 999-W
J. H. Christian, 999-W
C. L. Crawford, 773-42A
S. D. Fink, 773-A
K. M. Fox, 999-W
C. C. Herman, 773-A
E. N. Hoffman, 999-W
C. M. Jantzen, 773-A
F. C. Johnson, 999-W
J. C. Marra, 999-2W
D. H. McGuire, 999-W
D. H. Miller, 999-W
F. M. Pennebaker, 773-42A
W. R. Wilmarth, 773-A
Records Administration (EDWS)